

THE UNIVERSITY OF CALGARY

Fast Acting Load Control for Power System Stability

by

Kun Xiong

A THESIS

SUBMITTED TO THE FACULTY OF GRADUATE STUDIES
IN PARTIAL FULFILLMENT OF THE REQUIREMENTS FOR THE
DEGREE OF MASTER OF SCIENCE

DEPARTMENT OF ELECTRICAL AND COMPUTER
ENGINEERING

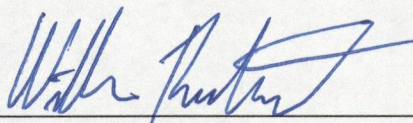
CALGARY, ALBERTA

August, 2003

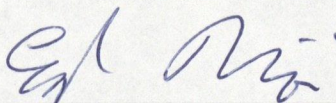
© Kun Xiong 2003

THE UNIVERSITY OF CALGARY
FACULTY OF GRADUATE STUDIES

The undersigned certify that they have read, and recommend to the Faculty of Graduate Studies for acceptance, a thesis entitled, "Fast Acting Load Control for Power System Stability" submitted by Kun Xiong in partial fulfillment of the requirements for the degree of Master of Science.



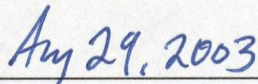
Supervisor, Dr. W. Rosehart
Dept. of Electrical and Computer Engineering



Dr. E. Nowicki
Dept. of Electrical and Computer Engineering



Dr. P. Goldsmith
Dept. of Mechanical and Manufacturing Engineering



Date

Abstract

Voltage stability is a subject of great concern in the planning and operation of power systems. As open access market principles are applied to power systems, stability margins have been reduced to respond to market pressures. This has lead to events such as rotating blackouts in several power systems, for example, California, and has generally resulted in increased electricity prices. A novel approach to reduce the tension in electrical systems is to establish a Fast Acting Load Control (FALC) program for price and system stability. Using this approach, load can be modelled and controlled similar to a generator, providing spinning reserve.

The thesis will review existing implementations of Fast Acting Load Control. Furthermore, in this thesis, two new Fast Acting Load Control procedures are proposed. One is a Lagrange Based Fast Acting Load Control, which is based on Lagrange multipliers to determine optimal locations and curtailment levels for voltage stability. Another procedure is Optimal Load Curtailment, which includes four techniques to determine the optimal load curtailment schemes for system and cost stability.

The effects of applying these approaches are analyzed using the IEEE 30-bus and IEEE 57-bus test systems.

Acknowledgements

I would like to express my appreciation for the supervision and guidance of Dr. William Rosehart and for the invaluable knowledge he has shared with me. My colleagues in the power group of University of Calgary were the sources of discussions and laughs.

My husband Wei Shen gave me countless understanding and support. The encouragement of my father Xiong, Jiancheng and my mother Peng, Zhifen from China has been greatly appreciated.

Table of Contents

Approval Page	ii
Abstract	iii
Acknowledgements	iv
Table of Contents	v
1 Introduction	1
1.1 Background	1
1.1.1 Fast Acting Load Control (FALC)	1
1.1.2 Power System Optimization	2
1.2 Research Motivation and Objectives	3
1.3 Implementation Methods	4
1.4 Outline of the Thesis	4
2 Power System Stability	7
2.1 Introduction	7
2.2 Small Signal Stability	8
2.2.1 Linearization	9
2.2.2 Eigenvalues and Eigenvectors	11
2.2.3 Eigenvalue and Stability	13
2.2.4 Small Signal Analysis Example	15
2.3 Bifurcation Analysis	17
2.3.1 Saddle-Node Bifurcations (SNB)	18
2.3.2 Limit-Induced Bifurcations (LIB)	19
2.3.3 Operating Limit Constrained Maximum Point	22
2.3.4 Bifurcation Analysis Methods	22
2.4 Optimization Techniques	26
2.4.1 Maximum Loadability Problem	26
2.5 Summary	29
3 Numerical Optimization	30
3.1 Introduction	30
3.1.1 Unconstrained Optimization	30
3.1.2 Constrained Optimization	33
3.2 Lagrange Methods	35

3.2.1	Lagrangian Function	35
3.2.2	Optimality Conditions	36
3.3	Lagrange Multiplier	37
3.3.1	Sensitivity with Linear Constraints	39
3.3.2	Sensitivity with Nonlinear Constraints	44
3.4	Interior Point Methods	46
3.4.1	Barrier Methods	46
3.4.2	Logarithmic-Barrier Interior Point Methods	48
3.4.3	Primal-Dual Interior Point Methods	51
3.5	Power System Analysis using Optimization Techniques	53
3.6	Summary	53
4	Lagrange based Fast Acting Load Control	55
4.1	Introduction	55
4.2	Lagrange Based Fast Acting Load Control	55
4.2.1	Single Curtailment Procedure (SCP)	56
4.2.2	Iterative Curtailment Procedure (ICP)	59
4.3	Numerical Analysis	60
4.3.1	Single Curtailment Procedure (SCP)	61
4.3.2	Iterative Curtailment Procedure (ICP)	63
4.4	Summary	69
5	Optimal Load Curtailment Program	70
5.1	Introduction	70
5.2	Improvement Based Load Curtailment Modelling	71
5.3	Generation Cost Minimization Optimal Power Flow	73
5.4	Optimal Load Curtailment	74
5.4.1	Fixed Generator Scheduling Technique (FGST)	77
5.4.2	Generator Active Power Distributed Technique (GAPDT)	78
5.4.3	Cost Constraint Technique (CCT)	80
5.4.4	Multi-Objective Technique (MOT)	81
5.5	Numerical Analysis	83
5.5.1	Fixed Generator Scheduling Technique (FGST)	83
5.5.2	Generator Active Power Distributed Technique (GAPDT)	87
5.5.3	Cost Constraint Technique (CCT)	87
5.5.4	Multi-Objective Technique (MOT)	89
5.5.5	Comparison of Results	93
5.6	Summary of Results	98
6	Conclusions	100

A List of Acronyms and Symbols	102
Bibliography	103

List of Tables

4.1	Maximum loading levels, λ_* , and desired maximum loading levels, λ_{desire} , of the modified system for IEEE 30-bus system	61
4.2	Stability Margin (MW) and Desired Stability Margin (MW) of the modified system by using Single Curtailment Procedure for IEEE 30-bus system	62
4.3	Maximum loading levels, λ_* , and desired maximum loading levels, λ_{desire} , of the modified system for IEEE 57-bus system	62
4.4	Stability Margin (MW) and Desired Stability Margin (MW) of the modified system by using Single Curtailment Procedure for IEEE 57-bus system	63
4.5	Amount of loads curtailed and iteration times for reaching the desired stability margin 400 MW , with different β	63
4.6	Amount of loads curtailed for reaching the desired stability margin 500 MW , with different β	64
5.1	The generator scheduling based on generator cost minimization OPF of IEEE 30-Bus System.	83
5.2	The generator active power reduced when the system choosing different slack bus.	84
5.3	The amount of total load in original system and the load curtailed to reach the stability margin 1000 MW by implementing FGAPT, CCT, GAPDT and MOT to IEEE 57-Bus System	96
5.4	The amount of total generator active power in original system and the generation reduction to reach the stability margin 1000 MW by implementing FGAPT, CCT, GAPDT and MOT to IEEE 57-Bus System	96
5.5	The generator cost after curtailing loads to reach the stability margin 1000 MW by the applying FGAPT, CCT, GAPDT and MOT to IEEE 57-Bus System	97

List of Figures

2.1	Generator connected to Infinite Bus system	15
2.2	Illustrative Diagram for Saddle-Node Bifurcations	19
2.3	Illustrative Diagram for Limit-Induced Bifurcations with unstable limit point	20
2.4	Illustrative Diagram for Limit-Induced Bifurcations with stable limit point	21
2.5	Illustrative Diagram for Operating Limit Constrained Maximum Point	23
2.6	Illustrate Diagram for continuation methods	25
3.1	Unconstrained local and global minima [31]	31
3.2	Plot of $g(x)$ for various values where $g(x) = x_1^2 + x_2^2$. The minimum is at the origin $(x_{1*}, x_{2*}) = (0, 0)$	32
3.3	Illustration of the minimum for function $g(x) = x_1^2 + x_2^2$ with constraint $x_1 + x_2 + 2 = 0$. The minimum is at $(x_{1*}, x_{2*}) = (-1, -1)$	34
3.4	Illustration of the Lagrange multiplier condition (3.17) for the problem $g(x) = x_1^2 + x_2^2$, and with constraint $x_1 + x_2 + 2 = 0$	38
3.5	Illustration of the sensitivity of Lagrange multipliers indicated in equation (3.32) for the problem $g(x) = x_1^2 + x_2^2$, and with constraint $x_1 + x_2 + 2 = 0$	43
4.1	Maximum loading level versus iteration times using ICP when the desired stability margin is 400 MW. The dotted, dashed, dashdot and solid lines correspond to $\beta = 2, 1, 0.5$ and 0.2 respectively.	65
4.2	Load curtailment on each bus using ICP when the desired stability margin is 400 MW, 500 MW and 700 MW.	66
4.3	Lagrange multipliers of each bus using ICP when the desired stability margin is 700 MW. The dash, dotted and solid lines correspond to iteration times = 1, 30 and 115 respectively.	67
4.4	The Comparison of ICP with different stability margin. The dotted, dashdot, dashed and big dotted correspond to stability margin = 400, 500, 600 and 700 respectively. The solid line indicates when 95 % of the desired stability margin is reached.	68
5.1	Illustration of Optimal Load Curtailment program with the stability margin in percentage. The solid and dashed lines represent the pre and after conditions of load curtailment respectively.	72

5.2	Illustration of Optimal Load Curtailment program with the stability margin in <i>MW</i> . The solid and dashed lines represent the before and after conditions of load curtailment respectively.	73
5.3	Illustration of Optimal Load Curtailment program.	77
5.4	Load curtailment versus stability margin using Fixed Generator Scheduling technique with different slack bus. The symbols \circ and $*$ correspond to solutions for the system choosing # 11 and # 13 bus as slack bus respectively.	85
5.5	Total generator cost versus stability margin using Fixed Generator Scheduling technique with different slack bus. The symbols \circ and $*$ correspond to solutions for the system choosing # 11 and # 13 bus as slack bus respectively.	86
5.6	Load curtailment versus stability margin using the Generator Active Power Distributed technique and Fixed Generator Scheduling technique with different slack buses. The symbols \triangleleft , \circ and $*$ correspond to solutions for the system using the Generator Active Power Distributed technique, Fixed Generator Scheduling technique choosing # 11 as slack bus and Fixed Generator Scheduling technique choosing # 13 bus as slack bus respectively.	88
5.7	Load curtailment versus stability margin using different cost control parameter β in Cost Constraint technique to IEEE 57-Bus test system. The symbols \circ , $*$ and \triangleleft correspond to solutions by using $\beta_c = 1, 0.99$ and 0.98 respectively.	90
5.8	Load curtailment versus stability margin using different weighting factors in Multi-Objective Technique to IEEE 57-Bus test system. The symbols $*$, \triangleleft and \diamond correspond to solutions by using $\omega_1 = 0.99, 0.5$ and 0.001 respectively.	91
5.9	Cost versus stability margin using different weighting factors in Multi-Objective Technique to IEEE 57-Bus test system. The symbols $*$, \triangleleft and \diamond correspond to solutions by using $\omega_1 = 0.99, 0.5$ and 0.001 respectively.	92
5.10	Load curtailment versus stability margin using different techniques to IEEE 57-Bus test system. The symbols $*$, \diamond , \circ and \triangleleft correspond to solutions by using Fixed Generator Scheduling, Generator Active Power Distributed, Cost Constraint and Multi-Objective techniques respectively.	94
5.11	Cost versus stability margin using different techniques to IEEE 57-Bus test system. The symbols $*$, \diamond , \circ and \triangleleft correspond to solutions by using Fixed Generator Scheduling, Generator Active Power Distributed, Cost Constraint and Multi-Objective techniques respectively.	95

5.12 Load curtailment versus stability margin using different techniques to IEEE 57-Bus test system. The symbols *, \diamond , \circ and \triangleleft correspond to solutions by using Fixed Generator Scheduling, Generator Active Power Distributed, Cost Constraint and Multi-Objective techniques respectively. The dotted line represents the solution by using Iterative Curtailment Procedure of LB-FALC.	98
---	----

Chapter 1

Introduction

1.1 Background

The application of open market principles to the operation of power systems has resulted in stability margins being reduced in response to market pressures [1]. Generally, the stability margin can be increased by having more spinning generation available to the system administrator, or by implementing Fast Acting Load Control schemes, in which some loads are treated as virtual generators that can be quickly curtailed [2].

1.1.1 Fast Acting Load Control (FALC)

Fast Acting Load Control can be defined as a load that can be curtailed quickly and directly by a system operator or a dispatcher without intervention of an operator at the end-use customer [3].

Due to the significant load growth and limited installation of new generation, various market operators have implemented load control programs to provide a venue for loads to compete with generation in the deregulated wholesale energy market. These programs provide an additional mechanism by which a proper load and resource balance might be maintained to avoid system reliability problem [4]. Various market operators have either implemented or considered implementing Fast Acting Load Control programs for system stability improvement.

Two trial demand response programs were implemented by the California Independent System Operator during the summer 2000 period [5]. The Alberta Electric System Operator (AESO) implemented a procurement of system load as an ancillary service to procure reserves in order to ensure continued system reliability and put downward pressure on ancillary services costs [6]. Also in 2001, the New York Independent System Operator implemented two programs aimed at increasing the opportunities for interruptible load and standby generation to participate in the New York wholesale electricity market [7].

Furthermore, the potential benefits of implementing load control schemes are explored in [8]. The load control scheme in [8] allows consumers to shift load from high priced hours to low priced hours during the day. The benefits to the individual consumer are explored through an example applied to residential air conditioning using price and demand data from California.

1.1.2 Power System Optimization

Optimization techniques are widely implemented in power system analysis and planning.

The Optimal Power Flow (OPF) problem, first formulated by Carpentier in 1962 [1] is a typical implementation of optimization techniques in power systems. Many voltage collapse problems can be restated and analyzed as optimization problems [9]. The applications of optimization techniques to voltage collapse analysis are discussed in many papers [10]-[11]. Also, Lagrange multiplier based optimization techniques have been used in several power system problems, including determining reserve allocation [12] and reducing power losses and the associated costs in the distribution

system [3].

Furthermore, Interior Point Methods (IPM) are powerful tools for solving many linear and nonlinear power system optimization problems such as transmission planning [13] and reactive power optimization [14].

This thesis applies numerical optimization techniques to Fast Acting Load Control to determine the load curtailment schemes to enhance system security and improve the stability margin of the system.

1.2 Research Motivation and Objectives

When power systems can not operate with large enough stability margins, instability problems can occur. Several voltage collapse events happened throughout the world [15]-[16] indicating systems are being operated with reduced stability margins. Thus, the development of effective approaches to enhance stability margin is necessary. Fast Acting Load Control is one of approaches to improve system stability margin.

The main motivation of the thesis is to provide a control scheme, which can determine the optimal locations and the amount of loads that should be curtailed to meet stability margin requirements.

The main objectives of the thesis research are as follows:

- Development of Maximum Loadability formulations that incorporate system loading ability to consider the influence of the stability margin on the OPF problems.
- Development of Optimal Load Curtailment formulations that determine the location that has the greatest effect to the system stability.

- Determination of the amount of loads that should be curtailed to meet the stability margin requirement.
- Implementation of the proposed formulations by testing them using several systems to analyze their feasibility and characteristics.

1.3 Implementation Methods

The proposed techniques are implemented using a combination of AMPL [17] and MATLAB [18] programming. AMPL is a modeling language, which is employed to develop and apply mathematical programming models [17]. The set of equations describing the objective and constraints of the system are modeled using AMPL. The optimization results from AMPL are modified into MATLAB format using a script file, and MATLAB routines are written to load the data files and generate the required vectors and matrices for numerical analysis. The software package LOQO [19] is used to solve the optimization problems. LOQO is based on Interior Point Optimization methods which tend to be well suited for power system problems [20].

1.4 Outline of the Thesis

The remaining chapters of the thesis are organized as follows:

Chapter 2 provides a brief review of power system stability problems. This is followed by an introduction to small signal stability and bifurcation analysis. Two types of bifurcations, Saddle-Node and Limit-Induced bifurcations, along with Operating Limit Constrained Maximum Point are introduced to analyze a system stability problem. Finally, a formulation of the Maximum Loadability problem is provided.

Chapter 3 reviews unconstrained and constrained optimization problems, along with a detailed derivation of the relationship between Lagrange multipliers, the objective function and constraints in an optimization problem. An interpretation of Lagrange multipliers is then presented. Next, an introduction to the Interior Point Method used to solve power system optimization problem is given.

Chapter 4 presents a Lagrange based Fast Acting Load Control technique, which is one of the main research contributions of this thesis. The technique uses numerical optimization techniques and Lagrange multipliers to determine which buses are having the greatest impact on stability and also determine the amount of load that should be curtailed. An analysis of the results obtained from applying the techniques to the IEEE 30-Bus and 57-Bus test systems is provided.

Chapter 5 presents the remaining research contributions of the thesis. Based on the Generation Cost Minimization Optimal Power Flow and Optimal Load Curtailment formulations, four techniques are introduced to determine load curtailment schemes for stability and generation cost optimization. The simulation results from implementing the formulations to two test systems are analyzed and the four techniques are compared.

Chapter 6 summarizes the work presented in the thesis. A summary of the main contributions of the thesis is given.

Chapter 2

Power System Stability

2.1 Introduction

Power System Stability may be defined as a property of the power system to regain an acceptable operating point or reach a new operating point of equilibrium after being subjected to a disturbance [21]. Stability analysis is very important for ensuring normal operation of a power system.

Stability in a power system may depend on many factors, such as the system configuration, operating mode, the size of disturbance and the period of time enduring disturbance.

If a sudden change or a sequence of changes occurs in one or more of the parameters of the power system, then the system is undergoing a disturbance.

Disturbances can be classified as either large disturbances or small disturbances. Large disturbances can include transmission system faults or loss of generation where the operating point moves far away from an equilibrium point. Therefore, the effect and stability of large disturbances is analyzed by nonlinear equations that describe the dynamics of the power system. Often, large disturbances are studied in transient stability analysis. If the power system undergoes changes that can be analyzed by linearized dynamic and algebraic equations, then it can be said that a small disturbance occurred. The daily change of loads is an example of a small disturbance. Linearized models of the system are valid when the operating points are 'close' to

equilibrium points. The space that can be defined as ‘close’ in general can not be explicitly defined.

Instability in a power system may be manifested in many different ways. The ability of power system to maintain steady acceptable voltages at all buses can be defined as *Voltage Stability* [22]. Traditionally, voltage stability includes large-disturbance voltage stability and small-disturbance voltage stability [21]. *Angle Stability* is the ability of interconnected synchronous machines of a power system to remain in synchronism, which generally includes small signal stability and transient stability [21].

In power system analysis, it is convenient to normalize system variables by using a per unit (*p.u.*) system, which may simplify computation by eliminating units. Therefore, some variables are expressed by the per unit system in this thesis.

In this chapter, the fundamental aspects of small signal stability are introduced. Also, this chapter presents analytical techniques for the study of small signal stability and small-disturbance voltage stability. Existing optimization techniques for the analysis of small-disturbance voltage stability problems are presented.

2.2 Small Signal Stability

Small signal stability is the ability of the power system to remain in synchronism when subjected to a small disturbance. From the definition of small disturbances, the disturbances are considered to be small enough that the equations describing the system models may be linearized [21]. Therefore, a linear approximation of the system can be used to determine the small signal stability.

One important small signal analysis method is investigating eigenvalues of the

linearized system.

2.2.1 Linearization

A system model may be represented by Differential and Algebraic Equations (DAE):

$$\dot{\mathbf{x}} = \mathbf{f}(\mathbf{x}, \mathbf{y}) \quad (2.1)$$

$$\mathbf{0} = \mathbf{g}(\mathbf{x}, \mathbf{y}) \quad (2.2)$$

where $\mathbf{x} \in \mathbb{R}^n$ is the vector of differential variables, $\mathbf{y} \in \mathbb{R}^m$ is the vector of algebraic variables, $\mathbf{f} \in \mathbb{R}^n$ and $\mathbf{g} \in \mathbb{R}^m$ are nonlinear equations.

To linearize equation (2.1) and (2.2), let \mathbf{x}_0 be the vector of differential states and \mathbf{y}_0 the vector of algebraic states corresponding to the equilibrium point around which the small signal performance is to be investigated. By definition, an equilibrium point is a solution of equations (2.1) and (2.2), where the system is at rest, i.e:

$$\dot{\mathbf{x}} = \mathbf{0} \quad (2.3)$$

Therefore

$$\mathbf{0} = \mathbf{f}(\mathbf{x}_0, \mathbf{y}_0) \quad (2.4)$$

$$\mathbf{0} = \mathbf{g}(\mathbf{x}_0, \mathbf{y}_0) \quad (2.5)$$

Assume the system has undergone a disturbance from the equilibrium point, the new operating point is defined as:

$$\mathbf{x} = \mathbf{x}_0 + \Delta \mathbf{x}$$

$$\mathbf{y} = \mathbf{y}_0 + \Delta \mathbf{y}$$

where the prefix Δ denotes a small deviation.

Since the new point must satisfy equation (2.1):

$$\dot{\mathbf{x}} = \dot{\mathbf{x}}_0 + \Delta\dot{\mathbf{x}} \quad (2.6)$$

$$= \mathbf{f}[(\mathbf{x}_0 + \Delta\mathbf{x}), (\mathbf{y}_0 + \Delta\mathbf{y})] \quad (2.7)$$

As the disturbance is assumed to be small, the nonlinear functions $\mathbf{f}(\mathbf{x}, \mathbf{y})$ can be expressed in terms of lower terms of Taylor's series expansion. When the terms involving second and higher order powers of Δx and Δy are neglected, equations (2.6) and (2.7) can be written as:

$$\begin{aligned} \dot{\mathbf{x}} &= \dot{\mathbf{x}}_0 + \Delta\dot{\mathbf{x}} \\ &= \mathbf{f}[(\mathbf{x}_0 + \Delta\mathbf{x}), (\mathbf{y}_0 + \Delta\mathbf{y})] \\ &= \mathbf{f}(\mathbf{x}_0, \mathbf{y}_0) + \mathbf{D}_x\mathbf{f}(\cdot)\Delta\mathbf{x} + \mathbf{D}_y\mathbf{f}(\cdot)\Delta\mathbf{y} \end{aligned} \quad (2.8)$$

where $\Delta\mathbf{x} \in \Re^n$, $\Delta\mathbf{y} \in \Re^m$, $\mathbf{D}_x\mathbf{f}(\cdot) \in \Re^{n \times n}$, $\mathbf{D}_y\mathbf{f}(\cdot) \in \Re^{n \times m}$ and

$$\begin{aligned} \mathbf{D}_x\mathbf{f}(\cdot) &= \begin{bmatrix} \frac{\partial f_1}{\partial x_1} & \cdots & \frac{\partial f_1}{\partial x_n} \\ \frac{\partial f_2}{\partial x_1} & \cdots & \frac{\partial f_2}{\partial x_n} \\ \vdots & \ddots & \vdots \\ \frac{\partial f_n}{\partial x_1} & \cdots & \frac{\partial f_n}{\partial x_n} \end{bmatrix} \\ \mathbf{D}_y\mathbf{f}(\cdot) &= \begin{bmatrix} \frac{\partial f_1}{\partial y_1} & \cdots & \frac{\partial f_1}{\partial y_m} \\ \frac{\partial f_2}{\partial y_1} & \cdots & \frac{\partial f_2}{\partial y_m} \\ \vdots & \ddots & \vdots \\ \frac{\partial f_n}{\partial y_1} & \cdots & \frac{\partial f_n}{\partial y_m} \end{bmatrix} \end{aligned}$$

Since $\dot{\mathbf{x}}_0 = \mathbf{f}(\mathbf{x}_0, \mathbf{y}_0) = 0$, equation (2.8) can be re-written as:

$$\Delta\dot{\mathbf{x}} = \mathbf{D}_x\mathbf{f}(\cdot)\Delta\mathbf{x} + \mathbf{D}_y\mathbf{f}(\cdot)\Delta\mathbf{y} \quad (2.9)$$

In the same manner, the linearized approximation of (2.2) is:

$$0 = \mathbf{D}_x \mathbf{g}(\cdot) \Delta \mathbf{x} + \mathbf{D}_y \mathbf{g}(\cdot) \Delta \mathbf{y} \quad (2.10)$$

where $\mathbf{D}_x \mathbf{g}(\cdot) \in \Re^{m \times n}$ and $\mathbf{D}_y \mathbf{g}(\cdot) \in \Re^{m \times m}$

Rearranging equation (2.10), gives:

$$\Delta \mathbf{y} = -(\mathbf{D}_y \mathbf{g}(\cdot))^{-1} \mathbf{D}_x \mathbf{g}(\cdot) \Delta \mathbf{x} \quad (2.11)$$

where the inverse of $\mathbf{D}_y \mathbf{g}(\cdot)$ is assumed to exist. Substituting (2.11) into (2.9), gives:

$$\begin{aligned} \Delta \dot{\mathbf{x}} &= \mathbf{D}_x \mathbf{f}(\cdot) \Delta \mathbf{x} - \mathbf{D}_y \mathbf{f}(\cdot) (\mathbf{D}_y \mathbf{g}(\cdot))^{-1} \mathbf{D}_x \mathbf{g}(\cdot) \Delta \mathbf{x} \\ &= (\mathbf{D}_x \mathbf{f}(\cdot) - \mathbf{D}_y \mathbf{f}(\cdot) (\mathbf{D}_y \mathbf{g}(\cdot))^{-1} \mathbf{D}_x \mathbf{g}(\cdot)) \Delta \mathbf{x} \end{aligned} \quad (2.12)$$

Therefore, the linearized set of equations can be expressed in the form as follows:

$$\Delta \dot{\mathbf{x}} = \mathbf{A} \Delta \mathbf{x} \quad (2.13)$$

where $\mathbf{A} \in \Re^{n \times n}$ is equal to $\mathbf{D}_x \mathbf{f}(\cdot) - \mathbf{D}_y \mathbf{f}(\cdot) (\mathbf{D}_y \mathbf{g}(\cdot))^{-1} \mathbf{D}_x \mathbf{g}(\cdot)$.

2.2.2 Eigenvalues and Eigenvectors

Eigenvalues are a special set of scalars associated with a linear system of equations.

The eigenvalues of a matrix is given by the values of the scalar parameter η for which there exist solutions other than $\phi = 0$ to the equation:

$$\mathbf{A} \phi = \eta \phi \quad (2.14)$$

where \mathbf{A} is a $n \times n$ matrix and ϕ is a $n \times 1$ vector.

Generally, there are n eigenvalues $\eta = \eta_1, \dots, \eta_n$ of matrix \mathbf{A} . Each eigenvalue is paired with a corresponding right eigenvector. For any eigenvalue η_i , the eigenvector ϕ_i which satisfies equation (2.14)

$$\mathbf{A}\phi_i = \eta_i\phi_i \quad \forall i = 1, 2, \dots, n \quad (2.15)$$

In order to express the eigenproperties of \mathbf{A} briefly, the following matrices are introduced:

$$\Phi = \begin{bmatrix} \phi_1 & \phi_2 & \dots & \phi_n \end{bmatrix} \quad (2.16)$$

$$\Lambda = \begin{bmatrix} \eta_1 & 0 & \dots & 0 \\ 0 & \eta_2 & \dots & 0 \\ 0 & 0 & \dots & 0 \\ 0 & 0 & \dots & \eta_n \end{bmatrix} \quad (2.17)$$

where each of the matrices is $n \times n$ and Λ is a diagonal matrix with the eigenvalues η_1, \dots, η_n .

Assume Φ^{-1} exists, then \mathbf{A} can be transformed to the diagonal matrix Λ according to equation (2.15) as follows:

$$\mathbf{A}\Phi = \Phi\Lambda$$

$$\Rightarrow \Lambda = \Phi^{-1}\mathbf{A}\Phi \quad (2.18)$$

$$\Rightarrow \mathbf{A} = \Phi\Lambda\Phi^{-1} \quad (2.19)$$

where Λ is expressed as in equation (2.17), which is a diagonal matrix with eigenvalues η_1, \dots, η_n .

2.2.3 Eigenvalue and Stability

A linearized system model can be expressed as follows:

$$\Delta \dot{\mathbf{x}} = \mathbf{A} \Delta \mathbf{x} \quad (2.20)$$

where \mathbf{A} , in general, is non-diagonal.

From equation (2.19), the non-diagonal matrix \mathbf{A} can be transformed to a diagonal matrix $\mathbf{\Lambda}$. Therefore, equation (2.20) can be rewritten as:

$$\begin{aligned} \Delta \dot{\mathbf{x}} &= \mathbf{\Phi} \mathbf{\Lambda} \mathbf{\Phi}^{-1} \Delta \mathbf{x} \\ \Rightarrow \mathbf{\Phi}^{-1} \Delta \dot{\mathbf{x}} &= \mathbf{\Lambda} \mathbf{\Phi}^{-1} \Delta \mathbf{x} \end{aligned} \quad (2.21)$$

Assume a new vector \mathbf{z} related to the original vector $\Delta \mathbf{x}$ by the transformation:

$$\mathbf{z} = \mathbf{\Phi}^{-1} \Delta \mathbf{x} \quad (2.22)$$

$$\dot{\mathbf{z}} = \mathbf{\Phi}^{-1} \Delta \dot{\mathbf{x}} \quad (2.23)$$

Substituting equation (2.22) and (2.23) into (2.21), gives:

$$\dot{\mathbf{z}} = \mathbf{\Lambda} \mathbf{z} \quad (2.24)$$

where $\mathbf{\Lambda}$ is a diagonal matrix with the i^{th} diagonal term equal to the eigenvalue η_i .

Therefore, equation (2.24) represents n equations as follows:

$$\dot{z}_i = \eta_i z_i \quad (2.25)$$

with $i = 1, 2, \dots, n$.

The solution of equation (2.25) with respect to time t is:

$$z_i(t) = z_i(0) e^{\eta_i t} \quad (2.26)$$

where $z_i(0)$ is the initial value of z_i .

From equation (2.22), Δx is given by:

$$\Delta \mathbf{x}(t) = \Phi \mathbf{z}(t) \quad (2.27)$$

$$= [\phi_1, \dots, \phi_n] \mathbf{z}(t) \quad (2.28)$$

$$= [\phi_1, \dots, \phi_n] [z_1(t), \dots, z_n(t)]' \quad (2.29)$$

$$= \sum_{i=1}^n \phi_i z_i(0) e^{\eta_i t} \quad (2.30)$$

where $\phi_i \in \mathbb{R}^{n \times 1}$ is the i^{th} column vector of Φ as defined in equation (2.16).

By using c_i to represent the scalar $z_i(0)$, equation (2.30) can be written as:

$$\Delta \mathbf{x}(t) = \sum_{i=1}^n \phi_i c_i e^{\eta_i t} \quad (2.31)$$

From equation (2.31), the stability of the system can be determined by the eigenvalues as follows:

1. If the eigenvalue is real, the system has a non-oscillatory mode. A negative real eigenvalue denotes a decaying mode. The larger the eigenvalue's magnitude, the faster the decay. A positive real eigenvalue denotes instability.
2. If the eigenvalue is complex, conjugate pairs occur and the system has an oscillatory mode. For complex eigenvalues, if any real part of eigenvalues is positive, the system is unstable; If all the real parts of eigenvalues are negative, the system is stable.

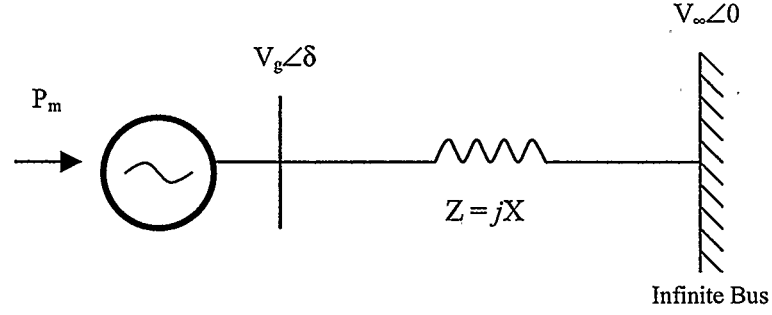


Figure 2.1: Generator connected to Infinite Bus system

2.2.4 Small Signal Analysis Example

The power system can be modeled by Differential-Algebraic Equations (DAE) as follows:

$$\dot{\mathbf{z}} = \mathbf{f}_d(\mathbf{z}, \mathbf{y}, \lambda) \quad (2.32)$$

$$0 = \mathbf{f}_a(\mathbf{z}, \mathbf{y}, \lambda) \quad (2.33)$$

where $\mathbf{z} \in \mathbb{R}^N$ is a vector of the differential variables, $\mathbf{y} \in \mathbb{R}^M$ is a vector of algebraic variables, and $\lambda \in \mathbb{R}$ is any parameter in the system that changes slowly.

A two-bus lossless system shown in Figure 2.1 is used to illustrate small signal analysis. From the classical model of generator, the system can be represented by equations as follows:

$$\dot{\delta} = \omega \quad (2.34)$$

$$\dot{\omega} = \frac{1}{H}(P_m - P_e - K_D \omega) \quad (2.35)$$

where P_m is mechanical power, P_e is electrical power, H is the inertia constant of the machine, K_D is the machine damping, ω is the difference from synchronous angular velocity of the generator rotor in electrical rad/s, and δ is the angular position of

the rotor in electrical radians with respect to a synchronously rotating reference. In this case, the mechanical power P_m is considered as the bifurcation parameter. The electrical power transmitted through the transmission line P_e is defined as:

$$P_e = \frac{|V_g||V_i|}{X} \sin \delta \quad (2.36)$$

where X is the transmission line impedance, $|V_g|$ is the magnitude of generator voltage, $|V_i|$ is the magnitude of the infinite bus voltage, which is a constant regardless of the power delivered to it or absorbed from it.

Let $H = 0.1$, $K_D = 0.1$, $X = 0.5$, $|V_g| = 1$ and $|V_i| = 1$, and substitute equation (2.36) into (2.35), then equations (2.34) and (2.35) can be re-written as:

$$\begin{bmatrix} \dot{\delta} \\ \dot{\omega} \end{bmatrix} = \begin{bmatrix} \omega \\ 10P_m - 20 \sin \delta - \omega \end{bmatrix} \quad (2.37)$$

The Jacobian of (2.37) with respect to $[\delta \ \omega]'$ is

$$\mathbf{J} = \begin{bmatrix} 0 & 1 \\ -20 \cos \delta & -1 \end{bmatrix} \quad (2.38)$$

Assume the system has undergone a disturbance from an equilibrium point (δ_0, ω_0) as:

$$\begin{aligned} \delta &= \delta_0 + \Delta\delta \\ \omega &= \omega_0 + \Delta\omega \end{aligned}$$

Therefore, the linearized model around equilibrium point (δ_0, ω_0) can be expressed as:

$$\begin{bmatrix} \dot{\Delta\delta} \\ \dot{\Delta\omega} \end{bmatrix} = \begin{bmatrix} 0 & 1 \\ -20 \cos \delta_0 & -1 \end{bmatrix} \begin{bmatrix} \Delta\delta \\ \Delta\omega \end{bmatrix} \quad (2.39)$$

Equation (2.39) is of the form $\Delta \dot{\mathbf{x}} = \mathbf{A} \Delta \mathbf{x}$. The eigenvalues of matrix \mathbf{A} can be obtained by solving the characteristic equation:

$$\begin{vmatrix} -\eta & 1 \\ -20 \cos \delta_0 & -1 - \eta \end{vmatrix} = 0 \quad (2.40)$$

or

$$\eta^2 + \eta + 20 \cos \delta_0 = 0 \quad (2.41)$$

The eigenvalues are

$$\eta_1, \eta_2 = -\frac{1}{2} \pm \frac{1}{2} \sqrt{1 - 80 \cos \delta_0} \quad (2.42)$$

Assume $\delta_0 \in \{0, \pi\}$, equation (2.42) gives:

1. When $\cos \delta_0 < 0$ i.e., $\frac{\pi}{2} < \delta_0 < \pi$, then $\eta > 0$ and the system is unstable.
2. When $\cos \delta_0 > 0$ i.e., $\delta_0 < \frac{\pi}{2}$, then $\eta < 0$ and the system is stable.
3. When $\cos \delta_0 = 0$ i.e., $\delta_0 = \frac{\pi}{2}$, then $\eta = 0$ and the system is at critical point between stable and unstable.

2.3 Bifurcation Analysis

Bifurcation analysis is used to describe how a system goes from being stable to unstable. If η_i are the eigenvalues of the linearized dynamic system model, the system can be described as follows:

1. If $Re[\eta_i] < 0$ for all i , the system is stable.
2. If $Re[\eta_i] > 0$ for all i , the system is unstable.

3. If $Re[\eta_i] = 0$ for any i , the system is going from stable to unstable (bifurcation point).

Several types of stability problems in power systems can be explained using bifurcation theory [23]. Bifurcation points can be defined as equilibrium points where changes in the ‘quantity’ and/or ‘quality’ of the equilibria associated with a nonlinear set of dynamic equations occur with respect to slow varying parameters in the system [24].

Saddle-Node Bifurcations (SNB) and Limit-Induced Bifurcations (LIB) are two typical types of bifurcations for analysis of power system. They are introduced in the following sections.

2.3.1 Saddle-Node Bifurcations (SNB)

Saddle-Node Bifurcations are characterized by the disappearance of a system equilibrium as parameters change slowly. Two equilibrium points, typically one stable and one unstable, merge at the bifurcation point.

In power systems, the Saddle-Node Bifurcation occurs when a stable operating equilibrium disappears. The consequence of the loss of the operating equilibrium can be voltage collapse. Therefore, Saddle-Node Bifurcations of power system models can be used to understand and analyze the voltage stability problem.

Figure 2.2 illustrates Saddle-Node Bifurcations of the two-bus lossless system shown in Figure 2.1. The equilibrium values of δ for different values of P_m are illustrated in Figure 2.2. When $P_m = 2.0$, the lower and upper curves merge, and no equilibrium exist for $P_m > 2.0$. The point at $P_m = 2.0$ is the saddle-node bifurcation point. In Figure 2.2, the upper branch corresponds to unstable equilibria and the

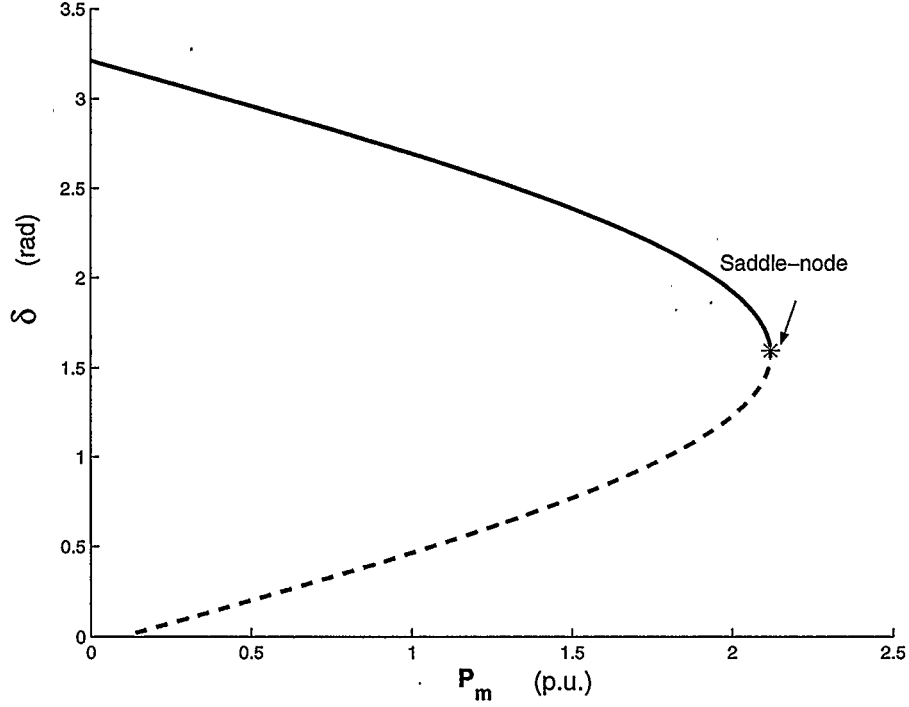


Figure 2.2: Illustrative Diagram for Saddle-Node Bifurcations

bottom branch corresponds to stable equilibria.

In a power system, the bifurcation parameter can be many factors, for example, the loading level and generator reactive power. As values in power systems are always restricted by operating limits, Limit-Induced Bifurcations are introduced in the following section.

2.3.2 Limit-Induced Bifurcations (LIB)

In power systems, control and/or operational limits have been shown to yield bifurcations known as Limit-Induced Bifurcations (LIB) [25]. As with SNB, LIB are also generic bifurcations. For example, when reactive power limits of certain generators are reached, the generator model is changed from constant voltage and active power

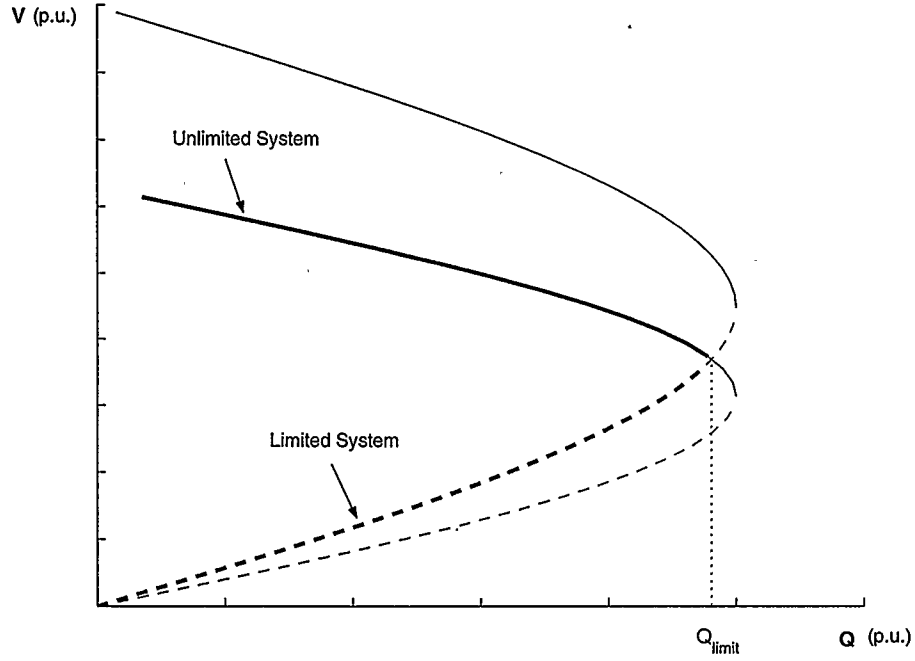


Figure 2.3: Illustrative Diagram for Limit-Induced Bifurcations with unstable limit point

model (PV), to constant active and reactive power model (PQ). There are two possible results when the reactive power limit is encountered. One is no local equilibria may exist for increased loading conditions [26] resulting in instability. Figure 2.3 shows this instability possibility. It is also possible that the system remains stable since the equilibrium point may be on the stable part of the Limit-Induced model's bifurcation diagram, and this possible result is shown in Figure 2.4.

The SNB/LIB point is also referred to as the voltage collapse point. At the point, the stability region of the system decreases until it becomes zero, resulting in a system collapse due to lack of equilibria. Thus, a voltage stability margin can be defined as the 'distance' from the present operating point to the voltage collapse or SNB/LIB point. The system is assumed to be voltage secure if this margin is reasonably greater

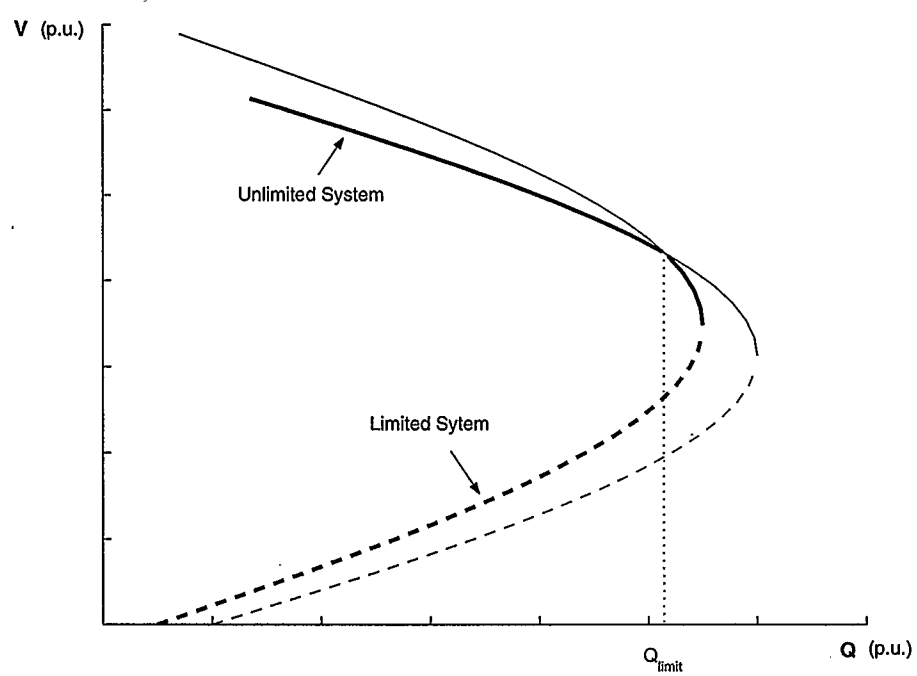


Figure 2.4: Illustrative Diagram for Limit-Induced Bifurcations with stable limit point

than zero. In practical systems, operators would be interested in maintaining the system with a given voltage stability margin, so that small disturbance do not make the system unstable [23].

2.3.3 Operating Limit Constrained Maximum Point

The Operating Limit Constrained Maximum Point is a critical point that is not related to stability problems in the network. Power systems have to be maintained within operating limits, for example there are strict rules on the magnitude of the bus voltages. Generally, the voltage magnitudes at each bus or node in the system must be always within a certain percentage of the nominal system voltage. Changes in loads, can result in situations where these limits are violated. If changes can not be made to independent variables to correct these violations, then corrective action such as load curtailment must be taken. Figure 2.5 shows the Operating Limit Constrained Maximum Point, which is not a bifurcation point.

2.3.4 Bifurcation Analysis Methods

Continuation and direct methods are two traditional methods for bifurcation analysis. The continuation method can be used to trace the set of equilibrium points the system goes through to arrive at the bifurcation point. For the saddle-node bifurcation, direct methods have been applied to determine the exact location of the saddle-node in power systems [27]-[28]. A brief review of these two bifurcation analysis methods is given in following sections.

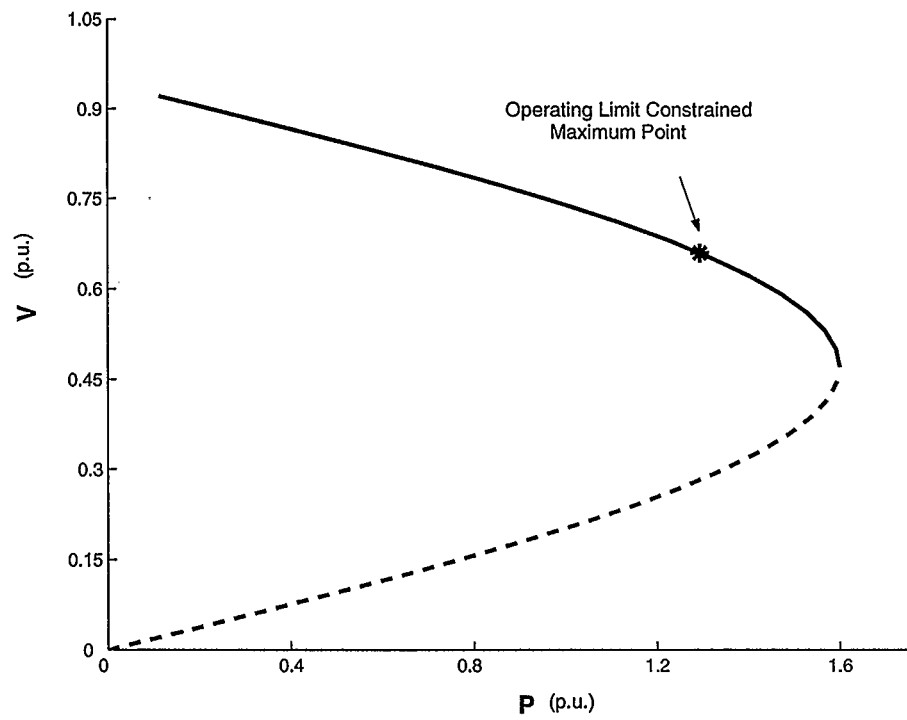


Figure 2.5: Illustrative Diagram for Operating Limit Constrained Maximum Point

Continuation Methods

In power systems, continuation methods can be used to trace the voltage profile up to the maximum loading point of the system. The advantage of the continuation method is a continuous voltage profile is traced and more information about the system behavior is obtained. However, the expensive computation cost is a disadvantage of this method.

Generally, continuation methods includes two or three steps:

1. **Predictor Step:** Start from an initial solution, use a tangent predictor to calculate the subsequent point corresponding to the incremental change in the bifurcation parameter. In this step, the estimated point on the predictor is not the real equilibrium point.
2. **Corrector Step:** Determine the real equilibrium point corresponding to the change in parameters.
3. **Parameterization Step:** Ensure that the Jacobian used in the continuation method does not become singular at a saddle-node bifurcation. This step can be omitted in some algorithms.

Figure 2.6 illustrates the predictor and corrector steps in continuation methods.

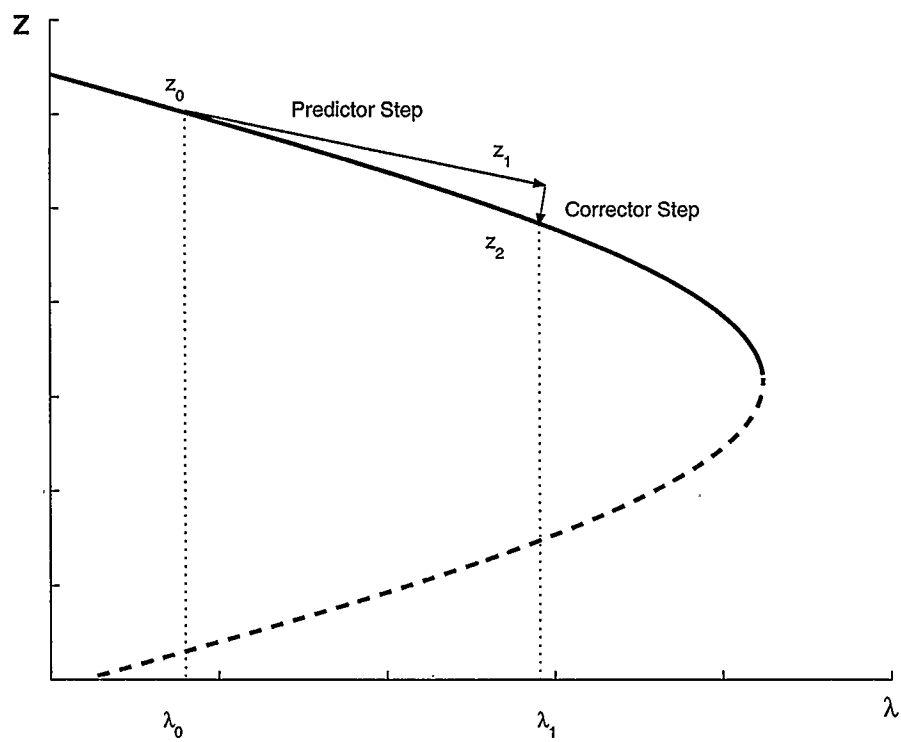


Figure 2.6: Illustrate Diagram for continuation methods

Direct Methods

Direct methods consist in solving the following set of equations to determine saddle-node bifurcations [29]:

$$s(\mathbf{z}_*, \lambda_*) = 0 \quad (2.43)$$

$$\mathbf{D}_{\mathbf{z}}^T s|_* \mathbf{w} = 0 \quad (2.44)$$

$$\|\mathbf{w}\|_{\infty} = 1 \quad (2.45)$$

where $\mathbf{D}_{\mathbf{z}}^T s|_*$ is the Jacobian of $s(\mathbf{z}_*, \lambda_*)$ and \mathbf{w} is a normalized right eigenvector of $\mathbf{D}_{\mathbf{z}}^T s|_*$.

2.4 Optimization Techniques

Based on bifurcation analysis methods, optimization techniques are introduced to analyze voltage stability and determine system settings to optimize power systems. In this section, the ‘Maximum Loadability’ (ML) problem is discussed.

2.4.1 Maximum Loadability Problem

In order to directly incorporate stability limits, a separate set of equations is defined to represent the system at the critical or maximum loading point [11, 30]. Using this approach, the constrained optimization problem (3.5) can be transformed into a ‘Maximum Loadability’ problem with constraints incorporated on the present and critical loading point [11, 30]. The Maximum Loadability problem can be written as

$$\begin{aligned}
& \max \quad \lambda_* - \lambda_p & (2.46) \\
& \text{s.t. :} \quad \mathbf{F}(\mathbf{x}_p, \boldsymbol{\rho}, \lambda_p) = \mathbf{0} \\
& \quad \mathbf{F}(\mathbf{x}_*, \boldsymbol{\rho}_*, \lambda_*) = \mathbf{0} \\
& \quad \underline{\mathbf{H}} \leq \mathbf{H}(\mathbf{x}_p, \boldsymbol{\rho}) \leq \overline{\mathbf{H}} \\
& \quad \underline{\mathbf{H}} \leq \mathbf{H}(\mathbf{x}_*, \boldsymbol{\rho}) \leq \overline{\mathbf{H}} \\
& \quad \underline{\mathbf{x}} \leq \mathbf{x} \leq \overline{\mathbf{x}} \\
& \quad \underline{\boldsymbol{\rho}} \leq \boldsymbol{\rho} \leq \overline{\boldsymbol{\rho}}
\end{aligned}$$

where the subscripts p and $*$ indicate the present and collapse points, respectively. $\mathbf{H}(\mathbf{x})$ usually represents transmission line limits, with lower and upper limits represented by $\underline{\mathbf{H}}$ and $\overline{\mathbf{H}}$, respectively. The lower and upper limits of the system variables \mathbf{x} are given by $\underline{\mathbf{x}}$ and $\overline{\mathbf{x}}$, respectively. Finally, $\boldsymbol{\rho}_* \supset \boldsymbol{\rho}$ is used to map the control variables at the present operating point into the maximum loading point to account for certain system changes. For example, generation levels at the present loading point are mapped to generation levels at the collapse point using a distributed slack bus. Thus, generators at the critical point are assumed to have the same terminal voltage set points as at the base loading point, and their power levels are represented based on the following distributed slack-bus model:

$$\mathbf{P}_{G*} = \mathbf{P}_{Gp}(1 + \mathbf{K}_{G*})$$

where \mathbf{K}_{G*} is a variable that distributes the generated powers at the critical point proportionally to the value of the independent control variable $\mathbf{P}_{Gp} \in \mathbf{x}_*$, i.e.

$$\mathbf{x}_* = [\delta_* \ \mathbf{V}_{L*} \ \mathbf{Q}_{G*} \ \mathbf{Q}_{S*}]^T$$

Hence,

$$\boldsymbol{\rho}_* = [\mathbf{P}_{G*}(\mathbf{P}_{Gp}, \mathbf{K}_{G*}) \mathbf{V}_{Gp} \mathbf{a}_p]^T$$

Observe that the tap settings \mathbf{a}_p are assumed to be the same for the present and maximum loading points.

The variable λ_* is a variable in the optimization problem, i.e. it is fully free to change during the solution process; on the other hand, λ_p is given a fixed value. Thus, the critical point is affected by changes in the control variables $\boldsymbol{\rho}$, due to the relationship between $\boldsymbol{\rho}$ and $\boldsymbol{\rho}_*$.

Furthermore, system load is modeled as constant PQ load as follows:

$$\mathbf{P}_l = \lambda \mathbf{P}_0$$

$$\mathbf{Q}_l = \lambda \mathbf{Q}_0$$

where $\lambda \in \{\lambda_p, \lambda_*\}$ is used to map the base load (P_0, Q_0) to the present and critical loading levels. Observe that in this case, λ_* stands for only one parameter instead of several, i.e. the load is assumed to change in only one known direction, which is a reasonable assumption based on an adequate load forecast at an ‘initial’ operating point \mathbf{x}_0 associated with λ_0 .

This problem maximizes the distance to a bifurcation or an operating limit constrained maximum. This distance may be defined as the stability margin. It is important to highlight the fact that in (2.46), the total generation at the critical operating point, is based on the generation at the present point and spinning reserve generation. Including the present loading point into the constraints ensures that, the feasibility and inequality constraints at the present loading point are met when

independent variables are calculated to maximize the distance to voltage collapse [11].

2.5 Summary

In this chapter, a review of power system stability is given. Small signal stability and bifurcation analysis are introduced to analyze the system stability. To determine the bifurcations, typical bifurcation analysis methods are presented. Based on these bifurcation analysis methods, a problem of maximizing the distance to voltage collapse is formulated by introducing optimization techniques. More detail about optimization techniques will be presented in the following chapter.

Chapter 3

Numerical Optimization

3.1 Introduction

Mathematical models of optimization can be generally represented by a constraint set \mathbf{X} and a cost function $g(\cdot)$ that maps elements of \mathbf{X} into real numbers [31]. The set \mathbf{X} consists of the available decisions \mathbf{X} and the cost $g(\mathbf{x})$ is a scalar measure of choosing decision \mathbf{x} . The optimal minimum is wanted, that is, an $\mathbf{x}_* \in \mathbf{X}$ such that

$$g(\mathbf{x}_*) \leq g(\mathbf{x}), \quad \forall \mathbf{x} \in \mathbf{X}$$

In subsequent sections, unconstrained and constrained optimization will be introduced.

3.1.1 Unconstrained Optimization

In this section, the following unconstrained optimization problem is considered:

$$\min g(\mathbf{x}) \quad \forall \mathbf{x} \in \mathbb{R}^n \tag{3.1}$$

Unconstrained Optimization problems are characterized by having an objective function but no constraints placed on the variables \mathbf{x} .

The following definitions are given to clarify the material presented in this chapter.

Global minimum is a point x_* such that

$$g(x_*) \leq g(x) \quad \forall x \in \mathbb{R}^n \tag{3.2}$$

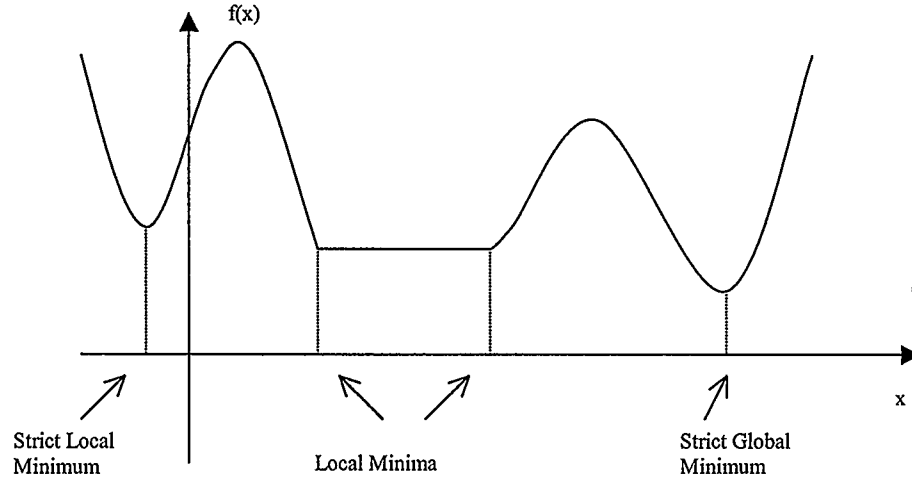


Figure 3.1: Unconstrained local and global minima [31]

Local minimum is a point x_* satisfying the condition that there is a $\varepsilon > 0$ such that

$$g(x_*) \leq g(x) \quad \forall \|x - x_*\| < \varepsilon \quad (3.3)$$

The unconstrained local or global minimum x_* is said to be strict if the corresponding inequality in (3.2) or (3.3) is strict for $x \neq x_*$. Otherwise, there are more than one x that let $g(x)$ be minimal. Figure 3.1 illustrates these definitions [31].

Gradient of $g(x)$ is a first-order differential operator that maps $g(x)$ to vector field. It is a n-vector expressed as:

$$\nabla g(\mathbf{x}) = \left(\frac{\partial g}{\partial x_1}, \dots, \frac{\partial g}{\partial x_n} \right) \quad (3.4)$$

To find the minimum of an unconstrained function, one of the general methods is setting $\frac{\partial g}{\partial x_*} = 0$. For example, given a function $g(x) = x_1^2 + x_2^2$. To find the minimum, set $\nabla g(x_*) = 0$, i.e. $\frac{\partial g}{\partial x_1} = 0$ and $\frac{\partial g}{\partial x_2} = 0$. Therefore, the function $g(x) = x_1^2 + x_2^2$ has the unique minimum of $g(x_*) = 0$ while $x_{1*} = 0$ and $x_{2*} = 0$. The graphic illustration is shown in Figure 3.2,

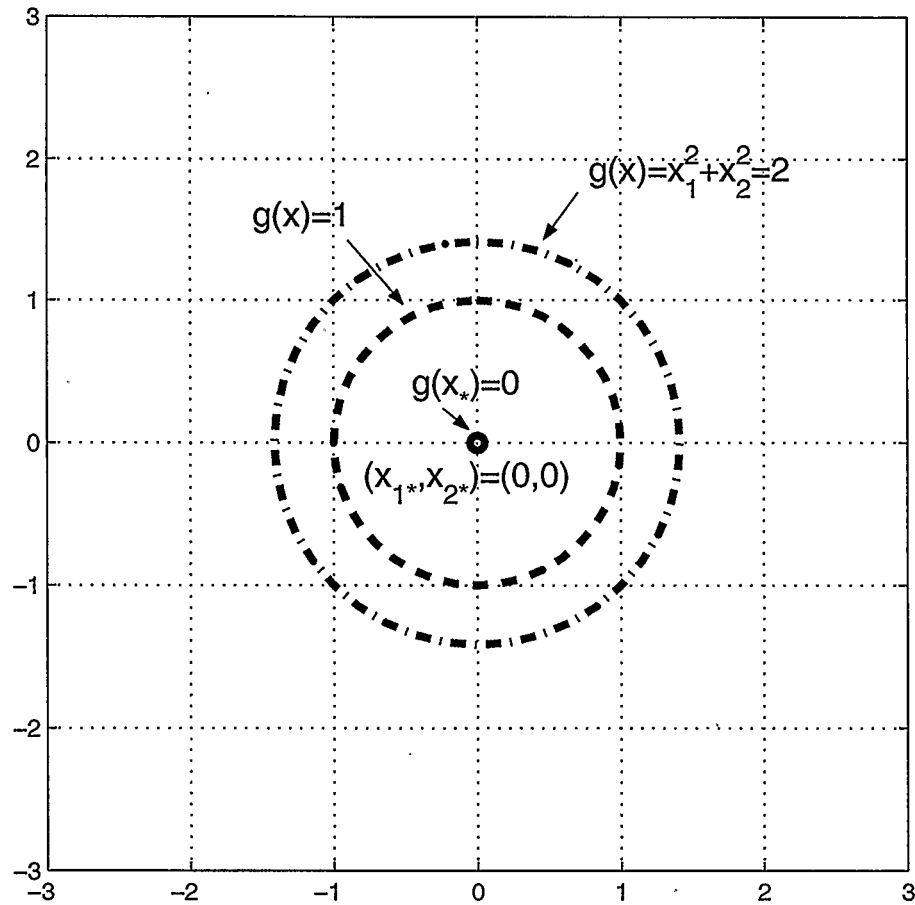


Figure 3.2: Plot of $g(x)$ for various values where $g(x) = x_1^2 + x_2^2$. The minimum is at the origin $(x_{1*}, x_{2*}) = (0,0)$

3.1.2 Constrained Optimization

Constrained Optimization problems are characterized by having an objective function and some equality and/or inequality constraints. Problems involving both equality and inequality constraints can be written as follows:

$$\begin{aligned} \min \quad & g(\mathbf{x}) \\ \text{s.t. :} \quad & \mathbf{F}(\mathbf{x}) = \mathbf{0} \\ & \underline{\mathbf{H}} \leq \mathbf{H}(\mathbf{x}) \leq \overline{\mathbf{H}} \end{aligned} \tag{3.5}$$

where $g(\mathbf{x})$ is the objective function or cost function, $\mathbf{F}(\mathbf{x})$ represents the equality constraint, $\mathbf{H}(\mathbf{x})$ represents the inequality constraint and *s.t.* is an acronym for *Subject to*.

For example, consider the function introduced in last section, $g(\mathbf{x}) = x_1^2 + x_2^2$ with the constraint $\mathbf{F}(\mathbf{x}) = x_1 + x_2 + 2 = 0$ added. The problem can be written as:

$$\begin{aligned} \min \quad & x_1^2 + x_2^2 \\ \text{s.t. :} \quad & x_1 + x_2 + 2 = 0 \end{aligned} \tag{3.6}$$

Without the constraint, the problem is an unconstrained optimization problem, and the minimum is at origin $(x_{1*}, x_{2*}) = (0, 0)$. However, the constrained minimum is at $(x_{1*}, x_{2*}) = (-1, -1)$. Figure 3.3 shows the graphic illustration of problem (3.6), where the dashed line represents the constraint function and the minimum for this constrained problem is at $x_{1*} = -1$ and $x_{2*} = -1$.

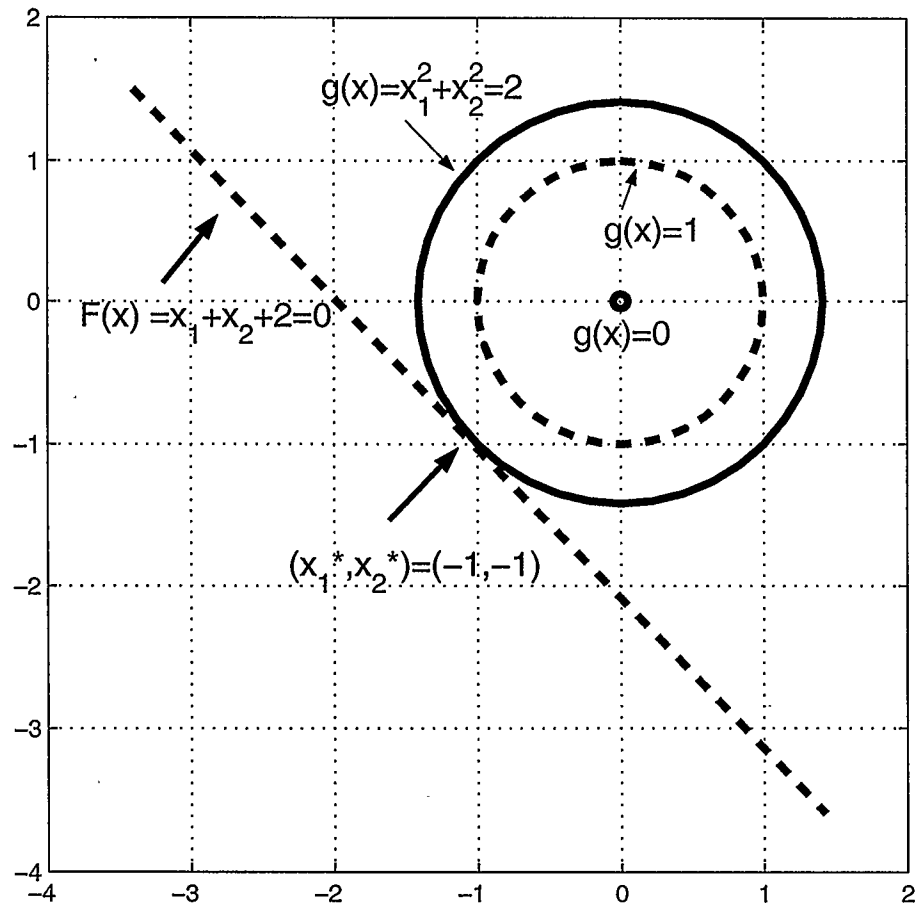


Figure 3.3: Illustration of the minimum for function $g(x) = x_1^2 + x_2^2$ with constraint $x_1 + x_2 + 2 = 0$. The minimum is at $(x_{1*}, x_{2*}) = (-1, -1)$

3.2 Lagrange Methods

The constrained optimization problem can be solved by many methods. One approach is to use the constraint to solve for one of the variables. For example, consider the problem in equation (3.6), use $x_2 = -2 - x_1$ and minimize the new function $f(x) = x_1^2 + (-2 - x_1)^2$. The difficulty with the above is that it is not always easy to solve explicitly for one of the variables. Therefore, another approach is the Lagrange method [32], which approaches the constrained optimization in a symmetric way almost like an optimization problem without constraints. In this section, Lagrange methods are firstly introduced. Then an interpretation of Lagrange Multipliers is presented.

In 1788, Lagrange discovered how to transform a constrained optimization problem, with equality constraints, into an unconstrained problem.

3.2.1 Lagrangian Function

The first step is forming the Lagrangian function. Assume a problem with equality constraints:

$$\begin{aligned} \min \quad & g(\mathbf{x}) \\ \text{s.t. : } & \mathbf{F}(\mathbf{x}) = \mathbf{0} \end{aligned} \tag{3.7}$$

where $\mathbf{F}(\mathbf{x}) : \Re^n \times \Re^m \rightarrow \Re^m$ and \mathbf{x} is a vector of n independent variables.

The Lagrangian function $L : \Re^{n+m} \rightarrow \Re$ is defined by:

$$L(\mathbf{x}, \boldsymbol{\gamma}) = g(\mathbf{x}) + \sum_{i=1}^m \gamma_i F_i(x)$$

where γ represent the Lagrange multipliers. Then, if \mathbf{x}_* is a local minimum, the equation (3.17) in Lagrange multiplier theorem can be written as [31]:

$$\nabla L(\mathbf{x}_*, \gamma_*) = \mathbf{0} \quad (3.8)$$

The next step is to minimize the unconstrained function $L(\mathbf{x}, \gamma)$ by solving the KKT (standing for ‘Karush-Kuhn-Tucker’) conditions $\nabla L(\mathbf{x}, \gamma) = \mathbf{0}$. The system of $(n + m)$ equations can be solved using Newton’s method.

3.2.2 Optimality Conditions

The Lagrangian function for inequality constrained optimization problem (3.5) can be written as follows:

$$L(\mathbf{x}, \gamma, \omega) = g(\mathbf{x}) + \gamma^T \mathbf{F}(\mathbf{x}) + \omega^T \mathbf{H}(\mathbf{x}) \quad (3.9)$$

where $\gamma \in \Re^m$ and $\omega \in \Re^p$ are Lagrange multipliers.

Let \mathbf{x}_* denote a point where the following conditions hold:

1. Feasibility:

$$\mathbf{F}(\mathbf{x}_*) = \mathbf{0} \quad (3.10)$$

$$\underline{\mathbf{H}} \leq \mathbf{H}(\mathbf{x}_*) \leq \overline{\mathbf{H}} \quad (3.11)$$

2. The first-order KKT conditions:

The terms ‘KKT point’ and ‘KKT conditions’ are used often. The first-order KKT conditions for the problem given in (3.5) hold at the point \mathbf{x}_* , or, equivalently, \mathbf{x}_* is a (first-order) KKT point, if there exist an m -vector γ_* and p -vector

ω_* , called a Lagrange multiplier vector, such that:

$$\mathbf{F}(\mathbf{x}_*) = \mathbf{0} \quad (\text{feasibility}) \quad (3.12)$$

$$\underline{\mathbf{H}} \leq \mathbf{H}(\mathbf{x}_*) \leq \overline{\mathbf{H}} \quad (\text{feasibility}) \quad (3.13)$$

$$\nabla_{\mathbf{x}, \gamma, \omega} L(\mathbf{x}_*, \gamma_*, \omega_*) = 0 \quad (\text{stationarity}) \quad (3.14)$$

$$\omega_* \geq 0 \quad (\text{multipliers nonnegativity}) \quad (3.15)$$

$$\mathbf{H}(\mathbf{x}_*) \cdot \omega_* = 0 \quad (\text{complementarity}) \quad (3.16)$$

It is common to refer to \mathbf{x} as the ‘primal variables’ and to the Lagrange multipliers γ and ω as the ‘dual variables’ [33].

3. **Constraint qualification:** The gradients of the constraints equal to zero at \mathbf{x}_* are linearly independent.

3.3 Lagrange Multiplier

The main Lagrange multiplier Theorem [31] can be presented as follows:

Let \mathbf{x}_* be a local minimum of $g(\mathbf{x})$ subject to $\mathbf{F}(\mathbf{x}) = 0$, and assume that the constraint gradients $\nabla F_1(\mathbf{x}_*), \dots, \nabla F_m(\mathbf{x}_*)$ are linearly independent. Then there exists a unique vector $\gamma_* = (\gamma_{1*}, \dots, \gamma_{m*})$, called a Lagrange multiplier vector or Lagrange multipliers, such that

$$\nabla g(\mathbf{x}_*) + \sum_{i=1}^m \gamma_{i*} \nabla F_i(\mathbf{x}_*) = 0 \quad (3.17)$$

Equation (3.17) can be interpreted as follows: the cost gradient $\nabla g(\mathbf{x}_*)$ belongs to the subspace spanned by the constraint gradients. To illustrate this, the constrained optimization problem (3.6) is considered again, and Figure 3.4 illustrates

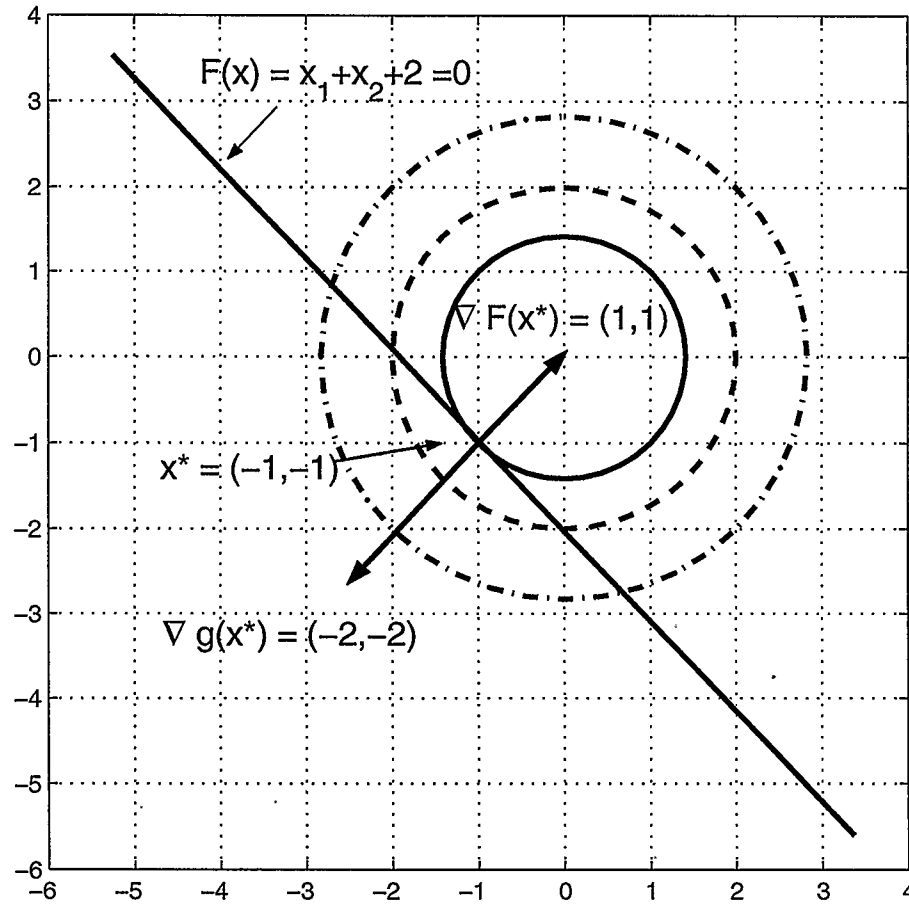


Figure 3.4: Illustration of the Lagrange multiplier condition (3.17) for the problem $g(x) = x_1^2 + x_2^2$, and with constraint $x_1 + x_2 + 2 = 0$.

this interpretation. As shown in the figure, at the local minimum $x_* = (-1, -1)$, the cost gradient $\nabla g(x_*)$ is normal to the constraint surface and is therefore, collinear with the constraint gradient $\nabla F(x_*) = (1, 1)$. The Lagrange multiplier is $\gamma = 2$.

To find critical points x_* of $g(x)$ subject to $F(x) = 0$ is equivalent to finding critical points (x_*, γ_*) of $L(x, \gamma)$. The unknown Lagrange multipliers γ_* accompany a critical point x_* of $g(x)$. Normally, the Lagrange multipliers are viewed as dual variables. They are not a part of the solution to the original problem, but has been

introduced as a convenience by which to arrive at that solution.

Moreover, Lagrange multipliers frequently have an interesting interpretation in specific practical contexts. In economic applications they can often be interpreted as prices, while in other problems they represent quantities with concrete physical meaning. Within the mathematical framework, they can be viewed as rates of change of the optimal cost as the level of constraint changes [31]. In other words, Lagrange multipliers represent local ‘prices’ associated with the right hand sides of the constraints. Therefore, they are very important in sensitivity analysis, such as cost *vs.* a budget or output *vs.* available material.

3.3.1 Sensitivity with Linear Constraints

Assume a problem involving a linear constraint as follows:

$$\min \quad g(\mathbf{x}) \quad (3.18)$$

$$\text{s.t. : } \mathbf{a}'\mathbf{x} = b \quad (3.19)$$

where $\mathbf{x} \in \mathbb{R}^n$. Given \mathbf{x}_* is a local minimum and γ_* is the corresponding Lagrange multipliers. If the level of constraint b is changed to $b + \Delta b$, the minimum \mathbf{x}_* will change to $\mathbf{x}_* + \Delta\mathbf{x}$, where $\Delta\mathbf{x}$ is undefined at the moment. Substituting $b \rightarrow b + \Delta b$ and $\mathbf{x}_* \rightarrow \mathbf{x}_* + \Delta\mathbf{x}$ into equation (3.19) gives:

$$\begin{aligned} \mathbf{a}'(\mathbf{x}_* + \Delta\mathbf{x}) &= b + \Delta b \\ \Rightarrow \mathbf{a}'\mathbf{x}_* + \mathbf{a}'\Delta\mathbf{x} &= b + \Delta b \end{aligned} \quad (3.20)$$

but from (3.19) $\mathbf{a}'\mathbf{x}_* = b$, so (3.20) can be re-written as

$$b + \mathbf{a}'\Delta\mathbf{x} = b + \Delta b \quad (3.21)$$

from (3.21), the variations $\Delta \mathbf{x}$ and Δb are related by

$$\mathbf{a}'\Delta \mathbf{x} = \Delta b \quad (3.22)$$

The Lagrangian function in this case is $L(\mathbf{x}, \gamma) = g(\mathbf{x}) + \gamma(\mathbf{a}'\mathbf{x} - b)$. So at the optimal point \mathbf{x}_* , using the Lagrange multiplier condition (3.12) gives:

$$\nabla_{\mathbf{x}}L(\mathbf{x}, \gamma) = 0 \quad (3.23)$$

$$\Rightarrow \nabla_{\mathbf{x}}g(\mathbf{x}_*) + \gamma_*\nabla_{\mathbf{x}}(\mathbf{a}'\mathbf{x} - b) = 0 \quad (3.24)$$

$$\Rightarrow \nabla_{\mathbf{x}}g(\mathbf{x}_*) + \gamma_*\mathbf{a}'\mathbf{I} = 0 \quad (3.25)$$

$$\Rightarrow \nabla_{\mathbf{x}}g(\mathbf{x}_*) = -\gamma_*\mathbf{a}'\mathbf{I} \quad (3.26)$$

where $\mathbf{I} := (1, \dots, 1)'$ is a vector of ones of n dimension. The change in the objective, $\Delta g(\mathbf{x}_*, \mathbf{x}_* + \Delta \mathbf{x})$, between the original optimal solution \mathbf{x}_* and the optimal solution to the new problem, corresponding to $b + \Delta b$ can be written as

$$\Delta g(\mathbf{x}_*, \mathbf{x}_* + \Delta \mathbf{x}) = g(\mathbf{x}_* + \Delta \mathbf{x}) - g(\mathbf{x}_*) \quad (3.27)$$

The Taylor series of $g(\mathbf{x}_* + \Delta \mathbf{x})$ is given by:

$$g(\mathbf{x}_* + \Delta \mathbf{x}) = g(\mathbf{x}_*) + \nabla_{\mathbf{x}}g(\mathbf{x}_*)'\Delta \mathbf{x} + \sigma(\|\Delta \mathbf{x}\|^2) \quad (3.28)$$

where $\sigma(\|\Delta \mathbf{x}\|^2)$ represents high order components. Substituting (3.28) into (3.27) gives:

$$\begin{aligned} \Delta g(\mathbf{x}_*, \mathbf{x}_* + \Delta \mathbf{x}) &= g(\mathbf{x}_*) + \nabla_{\mathbf{x}}g(\mathbf{x}_*)'\Delta \mathbf{x} + \sigma(\|\Delta \mathbf{x}\|^2) - g(\mathbf{x}_*) \\ &= \nabla_{\mathbf{x}}g(\mathbf{x}_*)'\Delta \mathbf{x} + \sigma(\|\Delta \mathbf{x}\|^2) \end{aligned} \quad (3.29)$$

Then substituting (3.26) into (3.29) gives:

$$\Delta g(\mathbf{x}_*, \mathbf{x}_* + \Delta \mathbf{x}) = -\gamma_*\mathbf{a}'\Delta \mathbf{x} + \sigma(\|\Delta \mathbf{x}\|^2) \quad (3.30)$$

Substituting (3.22) into (3.30) gives:

$$\Delta g(\mathbf{x}_*, \mathbf{x}_* + \Delta \mathbf{x}) = -\gamma_* \Delta b + \sigma(\|\Delta \mathbf{x}\|^2) \quad (3.31)$$

If the higher order components of (3.31) are assumed to be small enough to be ignored, i.e. $\sigma(\|\Delta \mathbf{x}\|^2) = 0$, an approximate relationship between the Lagrange Multiplier, γ_* , and the unit change in the objective function can be derived by rewriting (3.31):

$$\gamma_* \simeq -\frac{\Delta g(\mathbf{x}_*, \mathbf{x}_* + \Delta \mathbf{x})}{\Delta b} \quad (3.32)$$

Thus, the Lagrange multiplier γ_* gives the rate of optimal cost decrease when the level of constraint increases.

A similar procedure can be followed for the case of multiple constraints. In the case where there are multiple constraints $\mathbf{a}'_i \mathbf{x} = b_i$, $i = 1, \dots, m$, the preceding argument can be appropriately modified.

While constraints in this case become $\mathbf{a}'_i \mathbf{x} - b_i = 0$, $i = 1, \dots, m$, the Lagrangian function becomes:

$$L(\mathbf{x}, \boldsymbol{\gamma}) = g(\mathbf{x}) + \sum_{i=1}^m \gamma_i (\mathbf{a}'_i \mathbf{x} - b_i)$$

Then equations (3.23), (3.24) and (3.25) can be re-written as follows:

$$\nabla_{\mathbf{x}} L(\mathbf{x}_*, \boldsymbol{\gamma}_*) = 0 \quad (3.33)$$

$$\nabla_{\mathbf{x}} g(\mathbf{x}_*) + \sum_{i=1}^m \gamma_{i*} \nabla_{\mathbf{x}} (\mathbf{a}'_i \mathbf{x}_* - b_i) = 0 \quad (3.34)$$

$$\nabla_{\mathbf{x}} g(\mathbf{x}_*) + \sum_{i=1}^m \gamma_{i*} \mathbf{a}'_i \mathbf{I} = 0 \quad (3.35)$$

where $\mathbf{I} := (1, \dots, 1)'$ is a vector of ones of n dimension. Therefore,

$$\nabla_{\mathbf{x}} g(\mathbf{x}_*) = - \sum_{i=1}^m \gamma_{i*} \mathbf{a}'_i \mathbf{I} \quad (3.36)$$

Then substituting (3.36) into (3.29), the equation (3.30) can be modified as follows:

$$\begin{aligned}\Delta g(\mathbf{x}_*, \mathbf{x}_* + \Delta \mathbf{x}) &= \nabla_{\mathbf{x}} g(\mathbf{x}_*)' \Delta \mathbf{x} + \sigma(\|\Delta \mathbf{x}\|^2) \\ &= - \sum_{i=1}^m \gamma_{i*} \mathbf{a}_i' \Delta \mathbf{x} + \sigma(\|\Delta \mathbf{x}\|^2)\end{aligned}\quad (3.37)$$

While from equation (3.22), there is $\mathbf{a}_i' \Delta \mathbf{x} = b_i$, then equation (3.37) becomes:

$$\Delta g(\mathbf{x}_*, \mathbf{x}_* + \Delta \mathbf{x}) = - \sum_{i=1}^m \gamma_{i*} \Delta b_i + \sigma(\|\Delta \mathbf{x}\|^2) \quad (3.38)$$

Also, up to the first order, equation (3.38) can be written as follows:

$$\Delta g(\mathbf{x}_*, \mathbf{x}_* + \Delta \mathbf{x}) \simeq - \sum_{i=1}^m \gamma_{i*} \Delta b_i \quad (3.39)$$

To illustrate the interpretation of Lagrange multipliers in equation (3.39), the example in equation (3.6) is considered again. The optimal solution for this problem is $x_{1*} = -1, x_{2*} = -1$, with $\gamma_* = 2$. If the constraint changes on the right hand side, and becomes:

$$x_1 + x_2 + 2 = -1$$

The new right hand side is $\Delta b = -1$, so the approximate change in the cost is:

$$\Delta g \simeq -\gamma_* \Delta b = -2 * (-1) = 2 \quad (3.40)$$

Equation (3.40) states that the objective cost will increase by about 2 for a per unit decrease in the constraint. This is illustrated by Figure 3.5. The figure indicate that the local minimum is at $x_* = (-1, -1)$, and the Lagrange multiplier is $\gamma_* = 2$. When there is -1 change in the constraint, there is a χ increase in objective cost. The difference between χ and 2 is attributed to ignoring higher order terms in the derivation of equation (3.39).

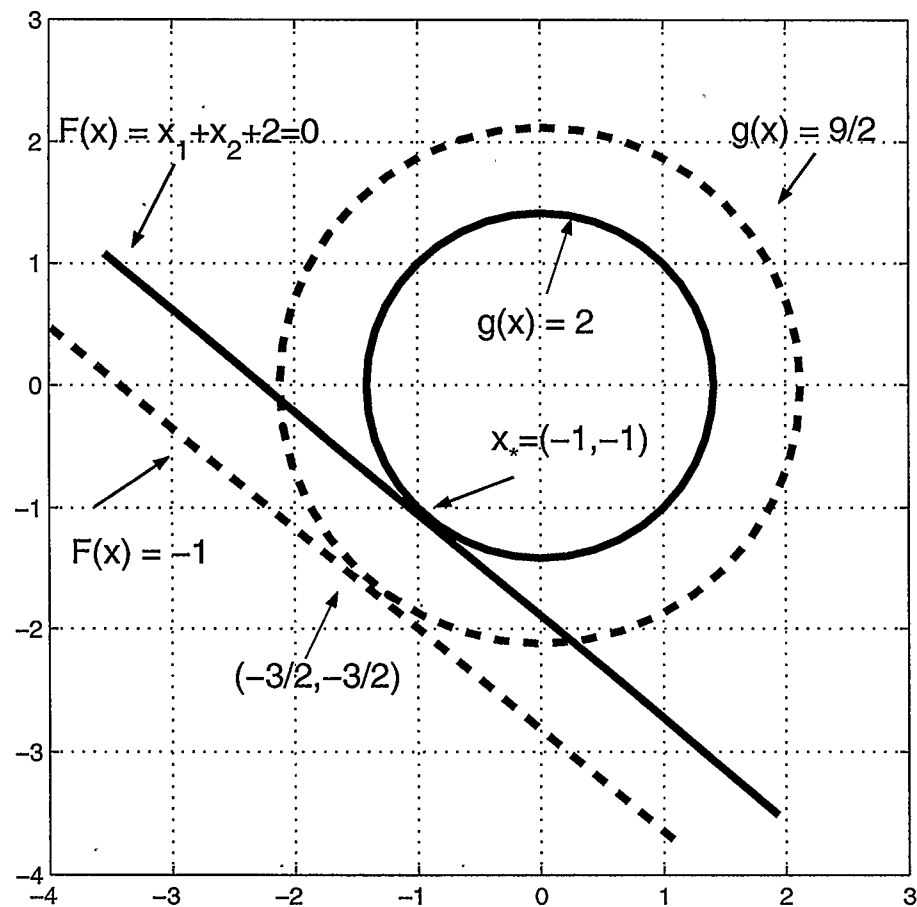


Figure 3.5: Illustration of the sensitivity of Lagrange multipliers indicated in equation (3.32) for the problem $g(x) = x_1^2 + x_2^2$, and with constraint $x_1 + x_2 + 2 = 0$.

3.3.2 Sensitivity with Nonlinear Constraints

This section provides an interpretation of Lagrange multipliers for the case of nonlinear constraints.

Given an optimization problem with an objective g and nonlinear constraints $\mathbf{F}(\cdot)$ as follows:

$$\begin{aligned} \min \quad & g(\mathbf{x}) \\ \text{s.t. : } & \mathbf{F}(\mathbf{x}) = \mathbf{u} \end{aligned} \tag{3.41}$$

where $\mathbf{F}(\cdot) : \mathbb{R}^n \times \mathbb{R}^m \rightarrow \mathbb{R}^m$ and $\mathbf{u} \in \mathbb{R}^m$ is a vector representing changes on the right hand side of the constraints. The Lagrangian function for (3.41) can be written as [33]:

$$L(\mathbf{x}, \boldsymbol{\gamma}) = g(\mathbf{x}) + \sum_{i=1}^m \gamma_i (F_i(\mathbf{x}) - \mathbf{u})$$

For $u = 0$, let \mathbf{x}_* , with the associated Lagrange multiplier vector $\boldsymbol{\gamma}_*$ be the solution to the local minimum. At the optimal point, the first order KKT conditions [33] are:

$$\begin{bmatrix} \nabla_{\mathbf{x}} L(\mathbf{x}_*, \boldsymbol{\gamma}_*) \\ \nabla_{\boldsymbol{\gamma}} L(\mathbf{x}_*, \boldsymbol{\gamma}_*) \end{bmatrix} = \begin{bmatrix} \nabla_{\mathbf{x}} g(\mathbf{x}_*) + \boldsymbol{\gamma}_*' \nabla_{\mathbf{x}} (\mathbf{F}(\mathbf{x}_*) - \mathbf{u}) \\ \mathbf{F}(\mathbf{x}_*) - \mathbf{u} \end{bmatrix} = \mathbf{0} \tag{3.42}$$

where $\boldsymbol{\gamma}_* \in \mathbb{R}^m$. Since \mathbf{u} is not a function of \mathbf{x} , the first term in (3.42) can be re-written as:

$$\nabla_{\mathbf{x}} g(\mathbf{x}_*) + \boldsymbol{\gamma}_*' \nabla_{\mathbf{x}} \mathbf{F}(\mathbf{x}_*) = \mathbf{0} \tag{3.43}$$

$$\Rightarrow \nabla_{\mathbf{x}} g(\mathbf{x}_*) = -\boldsymbol{\gamma}_*' \nabla \mathbf{F}(\mathbf{x}_*) \tag{3.44}$$

In order to demonstrate the relationship between the Lagrange multipliers and the objective function, a small non-zero value for \mathbf{u} is considered. Let $\mathbf{x} + \Delta \mathbf{x}$, with

corresponding Lagrange multiplier $\gamma + \Delta\gamma$, be the new local optimal solution. The difference between the original value of the objective function and the value at the new point is given by:

$$\Delta g(\mathbf{x}_*, \mathbf{x}_* + \Delta\mathbf{x}) = g(\mathbf{x}_* + \Delta\mathbf{x}) - g(\mathbf{x}_*) \quad (3.45)$$

Taking the Taylor series expansion of (3.45) around \mathbf{x}_* gives

$$\Delta g(\mathbf{x}_*, \mathbf{x}_* + \Delta\mathbf{x}) = g(\mathbf{x}_*) + \nabla_{\mathbf{x}} g(\mathbf{x}_*)' \Delta\mathbf{x} + \sigma(\|\Delta\mathbf{x}\|^2) - g(\mathbf{x}_*)$$

substituting (3.44) into the above and removing higher order terms gives:

$$\Delta g(\mathbf{x}_*, \mathbf{x}_* + \Delta\mathbf{x}) \simeq -\gamma_*' \nabla \mathbf{F}(\mathbf{x}_*)' \Delta\mathbf{x} \quad (3.46)$$

Similarly, the difference between the left hand side of the equality constraints for the original case and the new case, i.e. where $\mathbf{u} \neq \mathbf{0}$ can be written as:

$$\begin{aligned} \Delta \mathbf{F}(\mathbf{x}_*, \mathbf{x}_* + \Delta\mathbf{x}) &= \mathbf{F}(\mathbf{x}_* + \Delta\mathbf{x}) - \mathbf{F}(\mathbf{x}_*) \\ &\simeq \mathbf{F}(\mathbf{x}_*) + \nabla \mathbf{F}(\mathbf{x}_*)' \Delta\mathbf{x} - \mathbf{F}(\mathbf{x}_*) \\ &\simeq \nabla \mathbf{F}(\mathbf{x}_*)' \Delta\mathbf{x} \end{aligned} \quad (3.47)$$

Substituting the right hand side of (3.47) into (3.46) gives

$$\Delta g(\mathbf{x}_*, \mathbf{x}_* + \Delta\mathbf{x}) \simeq -\gamma_*' \Delta \mathbf{F}(\mathbf{x}_*, \mathbf{x}_* + \Delta\mathbf{x}) \quad (3.48)$$

Therefore, an approximate relationship between the Lagrange Multiplier, γ_* , and the change in the objective function can be derived by rearranging (3.48):

$$\gamma_* \simeq -\frac{\Delta g(\mathbf{x}_*, \mathbf{x}_* + \Delta\mathbf{x})}{\Delta \mathbf{F}(\mathbf{x}_*, \mathbf{x}_* + \Delta\mathbf{x})} \quad (3.49)$$

3.4 Interior Point Methods

Since Karmarkar's widely publicized announcement in 1984 of an interior point method [33], there has been extensive research into algorithms for linear and nonlinear programming that approach the solution through the interior of the feasible space.

The theoretical foundation for Interior Point (IP) methods fundamentally consists of three theories [34] :

1. Isaac Newton's method for solving nonlinear equations for unconstrained optimization;
2. Joseph Lagrange's methods for optimizations with equality constraints;
3. Anthony Fiacco and Garth McCormick's Barrier methods for optimizations with inequality constraints.

3.4.1 Barrier Methods

In the 1960s, the most popular approaches to solving constrained nonlinear optimization problems were based on Barrier methods, which have a common motivation: finding an unconstrained minima of a function that reflects the original objective function as well as the presence of constraints [33].

The idea of the barrier methods is to start from a point in the interior of the area defined by the inequalities and construct a barrier that prevents any variable from reaching the boundary. A barrier parameter is used to balance the contribution of the true objective function against that of the barrier function.

The Logarithmic-Barrier function, a composite based on the logarithmic interior function, is the overwhelmingly predominant barrier function employed today. Given a problem with inequality constraints:

$$\begin{aligned} \min \quad & g(\mathbf{x}) \\ \text{s.t. : } \quad & \mathbf{x} \geq \mathbf{0} \end{aligned} \tag{3.50}$$

The associated Logarithmic barrier function can be written as following:

$$B(\mathbf{x}, \mu) = g(\mathbf{x}) - \mu \sum_{i=1}^n (\log x_i) \tag{3.51}$$

where μ is a positive scalar, the barrier parameter. An important feature of $B(\mathbf{x}, \mu)$ is that it retains the smoothness properties of $g(\mathbf{x})$ and \mathbf{x} as long as $\mathbf{x} > \mathbf{0}$.

The problem (3.50) becomes an unconstrained problem as follows:

$$\min \quad g(\mathbf{x}) - \mu \sum_{i=1}^n (\log x_i) \tag{3.52}$$

As a simple example, consider the problem

$$\begin{aligned} \min \quad & (x_1 + 1)^2 + (x_2 - 1)^2 \\ \text{s.t. : } \quad & x_1 \geq 0 \\ & x_2 \geq 0 \end{aligned}$$

The unconstrained minimum is at $(x_{1*}, x_{2*}) = (-1, 1)$, but the constrained min-

imum is at $(x_{1*}, x_{2*}) = (0, 1)$. In this case, for any $\mu > 0$

$$\begin{aligned}
 B(x, \mu) &= (x_1 + 1)^2 + (x_2 - 1)^2 \\
 &\quad - \mu \log(x_1) - \mu \log(x_2) \\
 \frac{\partial B}{\partial x_1} &= 2(x_1 + 1) - \frac{\mu}{x_1} = 0 \\
 \frac{\partial B}{\partial x_2} &= 2(x_2 - 1) - \frac{\mu}{x_2} = 0 \\
 x_1 &= -\frac{1}{2} + \frac{1}{2}(1 + 2\mu)^{1/2} \\
 x_2 &= \frac{1}{2} + \frac{1}{2}(1 + 2\mu)^{1/2}
 \end{aligned}$$

which approaches $(0, 1)$ as $\mu \rightarrow 0$.

3.4.2 Logarithmic-Barrier Interior Point Methods

A brief review of the Logarithmic-Barrier IP methods can be written as following:

Step 1: Transform inequality constraints into equality constraints by introducing slack vectors \mathbf{s}_1 and \mathbf{s}_2 ;

Step 2: Put the nonnegativity constraints on the elements of \mathbf{s}_1 and \mathbf{s}_2 into the objective function using a logarithmic function;

Step 3: Introduce the barrier parameter μ , which is a constant and reduced after each iteration;

Step 4: Approximately solve the KKT conditions of the Lagrangian function;

Step 5: Update the variables and reduce the barrier function;

Step 6: Test for convergence. (If the solution meets the convergence criterion, optimal solution is found, otherwise go back to step 4.)

In this section, the steps in the Logarithmic-barrier IP method for Optimal Power Flow problem given above is presented in detail.

Assume a constrained problem with equality and inequality constraints:

$$\begin{aligned}
 \min \quad & g(\mathbf{x}) \\
 \text{s.t. :} \quad & \mathbf{F}(\mathbf{x}) = \mathbf{0} \\
 & \underline{\mathbf{H}} \leq \mathbf{H}(\mathbf{x}) \leq \overline{\mathbf{H}}
 \end{aligned} \tag{3.53}$$

The first step in solving (3.53) using the Logarithmic-Barrier IP method is to transform the existing inequality constraints into equality constraints by introducing strictly positive slack variables $\mathbf{s}_1, \mathbf{s}_2 \in \mathbb{R}^p$. Thus, the original problem can be rewritten as:

$$\begin{aligned}
 \min \quad & g(\mathbf{x}) \\
 \text{s.t. :} \quad & \mathbf{F}(\mathbf{x}) = \mathbf{0} \\
 & \mathbf{H}(\mathbf{x}) - \mathbf{s}_1 = \underline{\mathbf{H}} \\
 & \mathbf{H}(\mathbf{x}) + \mathbf{s}_2 = \overline{\mathbf{H}} \\
 & \mathbf{s}_1, \mathbf{s}_2 > \mathbf{0}
 \end{aligned} \tag{3.54}$$

From (3.54), in order to enforce the strict positivity constraints on \mathbf{s}_1 and \mathbf{s}_2 , an associated problem is formed by introducing a logarithmic barrier term written as following:

$$\begin{aligned}
 \min \quad & g(\mathbf{x}) - \mu^k \sum_{i=1}^p (\log s_1(i) + \log s_2(i)) \\
 \text{s.t. :} \quad & \mathbf{F}(\mathbf{x}) = \mathbf{0} \\
 & \mathbf{H}(\mathbf{x}) - \mathbf{s}_1 = \underline{\mathbf{H}} \\
 & \mathbf{H}(\mathbf{x}) + \mathbf{s}_2 = \overline{\mathbf{H}}
 \end{aligned} \tag{3.55}$$

where μ^k represents the positive barrier parameter at the k^{th} iteration. This parameter is approaching to zero as the iteration number k increases. To reduce the number of nonlinear terms, equation (3.55) can be re-written as follows:

$$\begin{aligned}
 \min \quad & g(\mathbf{x}) - \mu^k \sum_{i=1}^p (\log s_1(i) + \log s_2(i)) \\
 \text{s.t. :} \quad & \mathbf{F}(\mathbf{x}) = \mathbf{0} \\
 & \mathbf{s}_1 + \mathbf{s}_2 + \underline{\mathbf{H}} - \overline{\mathbf{H}} = \mathbf{0} \\
 & \mathbf{H}(\mathbf{x}) + \mathbf{s}_2 - \overline{\mathbf{H}} = \mathbf{0}
 \end{aligned} \tag{3.56}$$

For each fixed μ^k , the Lagrangian function $L_\mu(\mathbf{v})$ is defined as

$$\begin{aligned}
 L_\mu(\mathbf{v}) = \quad & g(\mathbf{x}) - \mu^k \sum_{i=1}^p (\log s_1(i) + \log s_2(i)) \\
 & + \gamma^T \mathbf{F}(\mathbf{x}) + \omega_1^T (\mathbf{s}_1 + \mathbf{s}_2 + \underline{\mathbf{H}} - \overline{\mathbf{H}}) \\
 & + \omega_2^T (\mathbf{H}(\mathbf{x}) + \mathbf{s}_2 - \overline{\mathbf{H}})
 \end{aligned} \tag{3.57}$$

where $\mathbf{v} := [\mathbf{x}; \mathbf{s}_1; \mathbf{s}_2; \gamma; \omega_1; \omega_2]$, $\gamma \in \Re^m$ and $\omega_1, \omega_2 \in \Re^p$ are Lagrange multipliers.

The first-order ‘KKT’ optimality conditions may be used to define the minimum of equation (3.57) with the following necessary conditions:

$$\nabla_{\mathbf{v}} L_\mu(\mathbf{v}) = \begin{bmatrix} \mathbf{D}_{\mathbf{x}} g(\mathbf{x}) - \mathbf{J}_{\mathbf{F}}(\mathbf{x})^T \gamma + \mathbf{J}_{\mathbf{H}}(\mathbf{x})^T \omega_2 \\ -\mu^k \mathbf{S}_1^{-1} \mathbf{I} + \omega_1 \\ -\mu^k \mathbf{S}_2^{-1} \mathbf{I} + (\omega_1 + \omega_2) \\ \mathbf{F}(\mathbf{x}) \\ \mathbf{s}_1 + \mathbf{s}_2 + \underline{\mathbf{H}} - \overline{\mathbf{H}} \\ \mathbf{H}(\mathbf{x}) + \mathbf{s}_2 - \overline{\mathbf{H}} \end{bmatrix} = \mathbf{0} \tag{3.58}$$

where $\mathbf{I} := (1, 1, 1, \dots, 1)^T$ is a vector of ones of the appropriate size, and $\mathbf{S}_1 = \text{diag}(\mathbf{s}_1)$ and $\mathbf{S}_2 = \text{diag}(\mathbf{s}_2)$. The function $\text{diag}(\mathbf{s}) : \mathbb{R}^p \rightarrow \mathbb{R}^{p \times p}$ represents a diagonal matrix with the i^{th} diagonal term equal to the i^{th} element in the vector \mathbf{s} , and $\mathbf{J}_{\mathbf{F}}(\mathbf{x}) \in \mathbb{R}^{m \times q}$ and $\mathbf{J}_{\mathbf{H}}(\mathbf{x}) \in \mathbb{R}^{p \times q}$ are the Jacobians of $\mathbf{F}(\mathbf{x})$ and $\mathbf{H}(\mathbf{x})$, respectively, i.e., $\mathbf{J}_{\mathbf{F}}(\mathbf{x}) = \mathbf{D}_{\mathbf{x}}\mathbf{F}(\mathbf{x})$ and $\mathbf{J}_{\mathbf{H}}(\mathbf{x}) = \mathbf{D}_{\mathbf{x}}\mathbf{H}(\mathbf{x})$. When the second term is scaled by \mathbf{S}_1 and the third by \mathbf{S}_2 , equation (3.58) can be rewritten as:

$$\nabla_v L_\mu(v) = \begin{bmatrix} \mathbf{D}_{\mathbf{x}}g(\mathbf{x}) - \mathbf{J}_{\mathbf{F}}(\mathbf{x})^T \boldsymbol{\gamma} + \mathbf{J}_{\mathbf{H}}(\mathbf{x})^T \boldsymbol{\omega}_2 \\ -\mu^k \mathbf{I} + \mathbf{S}_1 \boldsymbol{\omega}_1 \\ -\mu^k \mathbf{I} + \mathbf{S}_2 (\boldsymbol{\omega}_1 + \boldsymbol{\omega}_2) \\ \mathbf{F}(\mathbf{x}) \\ \mathbf{s}_1 + \mathbf{s}_2 + \underline{\mathbf{H}} - \overline{\mathbf{H}} \\ \mathbf{H}(\mathbf{x}) + \mathbf{s}_2 - \overline{\mathbf{H}} \end{bmatrix} = \mathbf{0} \quad (3.59)$$

3.4.3 Primal-Dual Interior Point Methods

In the past decade, Primal-Dual algorithms have emerged as the most important and useful algorithms from the interior-point class [31]. As in Primal-Dual methods for linear programming, the primal variables \mathbf{x} and the dual variables $\boldsymbol{\gamma}$ and $\boldsymbol{\omega}$ (representing the Lagrange multipliers) are treated as independent.

Assume a general constrained optimization problem as follows:

$$\begin{aligned} \min \quad & g(\mathbf{x}) \\ \text{s.t. :} \quad & \mathbf{F}(\mathbf{x}) = \mathbf{0} \\ & \underline{\mathbf{H}} \leq \mathbf{H}(\mathbf{x}) \leq \overline{\mathbf{H}} \end{aligned} \quad (3.60)$$

The Lagrangian function of the primal problem (3.60) is defined as

$$\begin{aligned} L(\mathbf{x}, \gamma, \omega_1, \omega_2) = & g(\mathbf{x}) + \gamma^T \mathbf{F}(\mathbf{x}) \\ & + \omega_1^T (\underline{\mathbf{H}} - \mathbf{H}(\mathbf{x})) + \omega_2^T (\mathbf{H}(\mathbf{x}) - \overline{\mathbf{H}}) \end{aligned} \quad (3.61)$$

where γ , ω_1 and ω_2 are Lagrange multipliers.

The dual function is defined as follows:

$$y(\gamma, \omega_1, \omega_2) = \inf_{\mathbf{x} \in \mathbf{X}} L(\mathbf{x}, \gamma, \omega_1, \omega_2) \quad (3.62)$$

Then the dual problem of (3.60) is:

$$\begin{aligned} \max \quad & y(\gamma, \omega_1, \omega_2) \\ \text{s.t. :} \quad & \omega_1, \omega_2 \geq 0 \end{aligned} \quad (3.63)$$

The Primal-Dual Interior Point Methods solve the primal and dual problems independently. The outline of the Primal-Dual IP methods is as the following:

Step 1: Initialization; (Choose a proper starting point such that the optimality conditions are satisfied.)

Step 2: Compute the barrier parameter, μ ;

Step 3: Solve the system of equations for primal and dual variables;

Step 4: Determine the step size and update the solutions;

Step 5: Convergence test. (If the solution meets the convergence criterion, the optimal solution is found, otherwise go back to step2)

The software package LOQO used to solve the optimization problems in this thesis implements a Primal-Dual Interior Point Method [19].

3.5 Power System Analysis using Optimization Techniques

In power system analysis, the Optimal Power Flow (OPF) problem has grown into a powerful tool for power system operation and planning. The OPF problem, first formulated by Carpentier in 1962, is a nonlinear programming problem that is used to determine the ‘optimal’ control parameter settings to minimize a desired objective function, subject to certain system constraints [35]. Depending on the definition of different objective functions, different Optimal Power Flow strategies can be pursued, and solutions to a variety of distinct problems can be obtained [36].

The OPF problem has been solved using a variety of nonlinear optimization techniques [35]. Interior Point methods are widely used tools for solving this problem, given their computational advantages when dealing with large systems that include a variety of operational and control limits [37].

The implementations of modified Interior Point Methods to solve power system optimization problems have been discussed recently [38]-[39].

3.6 Summary

In this chapter, methods of solving unconstrained and constrained optimization problems are presented. To solve the constrained optimization problems, Lagrange function and Lagrange multipliers are introduced. This is followed by a brief introduction of Lagrange methods, which transform the constrained optimization problem into an unconstrained problem. Also, the interpretation of Lagrange multipliers for sensitivity analysis is presented in this chapter. Next, a brief review of Interior Point methods is presented. This is followed by the derivation of the Logarithmic-Barrier

IP method and the introduction of the Primal-Dual IP method. The Primal-Dual IP method is implemented by the software package LOQO, which is used to solve the Optimal Power Flow problem in this thesis.

Chapter 4

Lagrange based Fast Acting Load Control

4.1 Introduction

Lagrange Based Fast Acting Load Control (LB-FALC) introduced in this chapter is used to determine which loads and how much load should be curtailed when the stability margin of the current operating point is lower than a desired value. The stability margin is increased by quickly decreasing the loading level in the system instead of by increasing spinning generation available to the system administrator.

The main focus of this chapter is on using numerical optimization techniques and Lagrange multipliers to determine, which buses are having the greatest impact on stability and also determine the amount of load that should be curtailed. Lagrange multiplier based optimization techniques have been used in several power system problems, including determining lost opportunity cost [12] and reducing power losses and the associated costs in the distribution system [3].

4.2 Lagrange Based Fast Acting Load Control

Since Lagrange Multipliers give an estimate of the effect of each of the constraints on the objective function, it is proposed that these multipliers be used to identify buses where loads are having the greatest impact on system stability and/or cost. One disadvantage of using Lagrange multipliers is that they are only an estimate.

Furthermore, if you make any changes in the system, for example, curtail load at a particular bus, the multipliers no longer provide relevant information, since the system has changed.

Based on the above discussion, two Lagrange based Load Curtailment technologies have been developed

1. **Single Curtailment Procedure (SCP)**: Use the Lagrange Multipliers to identify the bus that has the greatest effect on the system stability, and make a single reduction in load.
2. **Iterative Curtailment Procedure (ICP)**: Use an iterative approach. At each iteration, use the Lagrange Multipliers to identify the bus that has the greatest effect on the system stability.

4.2.1 Single Curtailment Procedure (SCP)

The main steps in the Single Curtailment Procedure are as follows:

1. Solve the Maximum Loadability (ML) problem.
2. Check the Lagrange Multipliers, and find the maximum to identify the bus that has largest impact on the loadability of the system.
3. Curtail the load at the identified bus according to the following formula:

$$P_{new(i)} = (1 - k)P_{0(i)} \quad (4.1)$$

where P_{new} is the new active power of the load, P_0 is original active power of the load, i is the bus identified using the Lagrange Multipliers and k is the curtailment parameter representing the percent of load being curtailed.

For the above procedure, the challenge is to determine the curtailment parameter k . That means how much load should be curtailed to reach the desired loading level. The $\lambda_{desired}$ and Lagrange Multipliers are important factors to determine the parameter k .

Using the relationship between the Lagrange multipliers and the change in the objective function presented in Chapter 3, the parameter k in equation (4.1) is determined.

Assuming an initial solution, $\{x_*, \lambda_*\}$ to the Maximum Distance to Collapse problem is found, where λ_* is less than a desired value, $\lambda_{desired}$. The largest Lagrange multiplier is used to identify the bus having the greatest impact on the stability margin. This bus is then selected for load curtailment. The difference between the initial value of λ_* and the desired value can be expressed as a difference in the objective function between the original case and the case where load has been curtailed:

$$\begin{aligned}
 \Delta g(x_*, x_* + \Delta x) &= g(x_* + \Delta x) - g(x_*) \\
 &= -(\lambda_{desired} - \lambda_p) - (-(\lambda_* - \lambda_p)) \\
 &= -(\lambda_{desired} - \lambda_*)
 \end{aligned} \tag{4.2}$$

The change in the right hand side of the load flow equation identified as having the biggest impact on the stability margin before and after load curtailment is:

$$\Delta F(x_*) = -(\lambda_{desired} P_{new} - \lambda_* P_0) \tag{4.3}$$

where P_{new} , and P_0 are the new and old active power of the load at the identified bus respectively. Substituting (4.1) into (4.3), gives:

$$\begin{aligned}\Delta F(x_*) &= -(\lambda_{desire}(1-k)P_0 - \lambda_*P_0) \\ \Rightarrow \Delta F(x_*) &= -(\lambda_{desire} - \lambda_*)P_0 + \lambda_{desire}kP_0\end{aligned}\quad (4.4)$$

Equations (4.4) and (4.2) are substituted into (3.49), the expression found in Chapter 3, that relates the Lagrange multiplier with the incremental change in the constraint and objective equations.

$$\gamma_* = -\frac{-(\lambda_{desire} - \lambda_*)}{-(\lambda_{desire} - \lambda_*)P_0 + \lambda_{desire}kP_0} \quad (4.5)$$

The following steps are then taken to re-write (4.5) as an explicit function of k .

$$\begin{aligned}\frac{1}{\gamma_*} &= -\frac{-(\lambda_{desire} - \lambda_*)P_0 + \lambda_{desire}kP_0}{-(\lambda_{desire} - \lambda_*)} \\ \Rightarrow \frac{1}{\gamma_*} &= \frac{-(\lambda_{desire} - \lambda_*)P_0 + \lambda_{desire}kP_0}{\lambda_{desire} - \lambda_*} \\ \Rightarrow \frac{1}{\gamma_*} &= -P_0 + \frac{\lambda_{desire}kP_0}{\lambda_{desire} - \lambda_*} \\ \Rightarrow \frac{1}{\gamma_*} + P_0 &= \frac{\lambda_{desire}kP_0}{\lambda_{desire} - \lambda_*} \\ \Rightarrow k &= \left(1 + \frac{1}{\gamma_*P_0}\right) \frac{\lambda_{desire} - \lambda_*}{\lambda_{desire}}\end{aligned}\quad (4.6)$$

Equation (4.6), which is used to determine how much load should be curtailed at the selected bus, can be interpreted along with (4.1) as follows:

- the reduction in load will have two components, one relating only to the difference between the desired maximum loading level and the initial maximum loading level and the other a function of the Lagrange multiplier and the loading levels.

- the amount of load curtailed is inversely proportional to the magnitude of the Lagrange multiplier. This intuitively makes sense, because if the Lagrange multiplier is large, then curtailing load at the bus, will have a large impact on the maximum loading level, so less load needs to be curtailed.

Because of the nonlinear nature of power systems, and the fact that the Lagrange multipliers give only an approximation of the effect of a constraint on the objective function in the global sense, the above procedure may not be effective when there is a large difference between the desired and initial maximum loading margin. This difference will be shown in the numerical analysis section.

4.2.2 Iterative Curtailment Procedure (ICP)

In order to compensate the local nature of Lagrange multipliers in nonlinear problems, an iterative procedure based on the method described in the previous section is proposed. The steps in the iterative procedure are as follows:

1. Solve the Maximum Loadability (ML) problem.
2. Check the Lagrange Multipliers, and find the maximum to identify the bus that has largest impact on the loadability of the system.
3. Curtail the load at the identified bus according to the following formula:

$$P_{new(i)} = (1 - k')P_{0(i)} \quad (4.7)$$

where P_{new} is the new active power of the load, P_0 is the original active power of the load, i is the bus identified using the Lagrange Multipliers and k' is the

curtailment parameter representing the percent of load being curtailed. The parameter k' is calculated as follows:

$$k' = \beta k \quad (4.8)$$

where β is a scaling factor and k is defined by (4.6). The value used for β will depend on the desired characteristics of the solution. Different choices for β are considered in the numerical simulations.

4. Resolve the Maximum Loadability problem.
5. If the value for λ_* is less than $\lambda_{desired}$ then repeat steps #2 through #4 until $\lambda_* \geq \lambda_{desired}$.

The advantage of the above procedure versus the single iteration procedure is that changes in the characteristics of the system that result from changes in loads are taken into account when determining the total amount of load that should be curtailed. This will tend to allow the problem to converge to a better or more optimal final solution.

4.3 Numerical Analysis

The proposed formulations presented in Section 4.2 are tested on sample systems based on the IEEE 30-bus and 57-bus test system [40]. The optimization problems are solved using the software package LOQO [19] and the modeling language AMPL [17]. LOQO is based on Interior Point Optimization methods which tend to be well suited for power system problems [20].

In the numerical simulations performed, two methods are used to interpret the desired stability margin $\lambda_{desired}$, as a percentage of the current loading level and also using total load active power (MW). Both approaches are taken because the distance to between the current load and the maximum loading point in terms of MW will change as load is curtailed when using the percentage method.

4.3.1 Single Curtailment Procedure (SCP)

The Single Curtailment Procedure is first applied to the IEEE 30-bus system. In Tables 4.1 and 4.2, the values of λ_* obtained when using different values of $\lambda_{desired}$ are given. For each case, the current loading level, i.e. λ_p , is fixed at one.

Present Loading Level	Maximum Loading Level	
λ_p (p.u.)	$\lambda_{desired}$ (p.u.)	λ_* (p.u.)
1.00	1.3	1.253
1.00	1.4	1.309
1.00	1.5	1.359
1.00	1.6	1.400
1.00	1.7	1.435
1.00	1.8	1.466

Table 4.1: Maximum loading levels, λ_* , and desired maximum loading levels, $\lambda_{desired}$, of the modified system for IEEE 30-bus system

Next, the Single Curtailment Procedure is applied to the IEEE 57-bus system.

Stability Margin (MW)	Desired Margin (MW)	Difference (MW)	Difference (%)
81.1	100	18.9	18.9
106.42	150	43.58	29.1
125.27	200	74.73	37.37
140.46	250	109.54	43.82
152.17	300	147.83	49.28

Table 4.2: Stability Margin (MW) and Desired Stability Margin (MW) of the modified system by using Single Curtailment Procedure for IEEE 30-bus system

A summary of the results are given in Tables 4.3 and 4.4.

Present Loading Level	Maximum Loading Level	
λ_p (p.u.)	λ_{desire} (p.u.)	λ_* (p.u.)
1.00	1.3	1.241
1.00	1.4	1.272
1.00	1.5	1.314
1.00	1.6	1.355
1.00	1.7	1.381
1.00	1.8	1.402

Table 4.3: Maximum loading levels, λ_* , and desired maximum loading levels, λ_{desire} , of the modified system for IEEE 57-bus system

The tables illustrates difference between the desired maximum loading level λ_{desire} and the real maximum loading level λ_* after load curtailment. From the tables, the following observations are made: When the value of λ_{desire} is low, the procedure tends to choose the amount of curtailment that allows the stability margin to approach the desired value. When the value of λ_{desire} is high, the difference between λ_* and λ_{desire} after applying the procedure tends to be large. This result can be ex-

Stability Margin (<i>MW</i>)	Desired Margin (<i>MW</i>)	Difference (<i>MW</i>)	Difference (%)
294.39	300	5.61	1.87
318.23	400	81.77	20.4
358.84	500	141.16	28.23
409.36	600	190.64	31.77
451.44	700	248.56	35.5

Table 4.4: Stability Margin (*MW*) and Desired Stability Margin (*MW*) of the modified system by using Single Curtailment Procedure for IEEE 57-bus system

plained because of the local nature of Lagrange multipliers, and the linear approach used to formulate the value of k , the curtailment parameter.

4.3.2 Iterative Curtailment Procedure (ICP)

The Iterative Curtailment Procedure is applied to IEEE 57-bus test case.

β	Load curtailed (<i>MW</i>)	Iteration number
2.00	1.677	16
1.00	1.6766	36
0.50	1.6766	75
0.20	1.6765	193

Table 4.5: Amount of loads curtailed and iteration times for reaching the desired stability margin 400 *MW*, with different β

Table 4.5 gives the size of load, in *MW*, that will be curtailed and the total number of iterations required to reach the desired stability margin 400 *MW* with different values of the parameter β . As expected, the rate of convergence is directly

proportional to the value of β . The advantage of using a smaller value of β is the procedure will tend to better select which loads would be curtailed and therefore the total amount of load curtailed will be reduced. The disadvantage is making β too large may result in excessive load curtailment. This disadvantage is illustrated in Table 4.6 which lists the excessive loads curtailed using different values of β . The curtailed loads are very close when choosing β 0.5, 1 and 2. However, if β is 8, a lot of excessive loads are curtailed, which reduces the accuracy of load curtailment program.

β	Load curtailed (MW)	Excessive load curtailed (MW)
0.5	3.55	0
1.00	3.56	0.01
2.00	3.57	0.02
5.00	3.86	0.31
8.00	5.8	2.25

Table 4.6: Amount of loads curtailed for reaching the desired stability margin 500 MW , with different β

Figure 4.1 is a plot of the value of λ_* at each iteration of the procedure using different values of the parameter β .

Unlike the Single Curtailment Procedure, the Iterative Curtailment Procedure tends to reach the desired stability margin. Figure 4.2 shows the load curtailment on each bus when the desired stability margin is 400 MW , 500 MW and 700 MW respectively. When the desired stability margin is 400 MW , the load curtailment is applied only on bus 31 to meet the required stability margin. However, when the

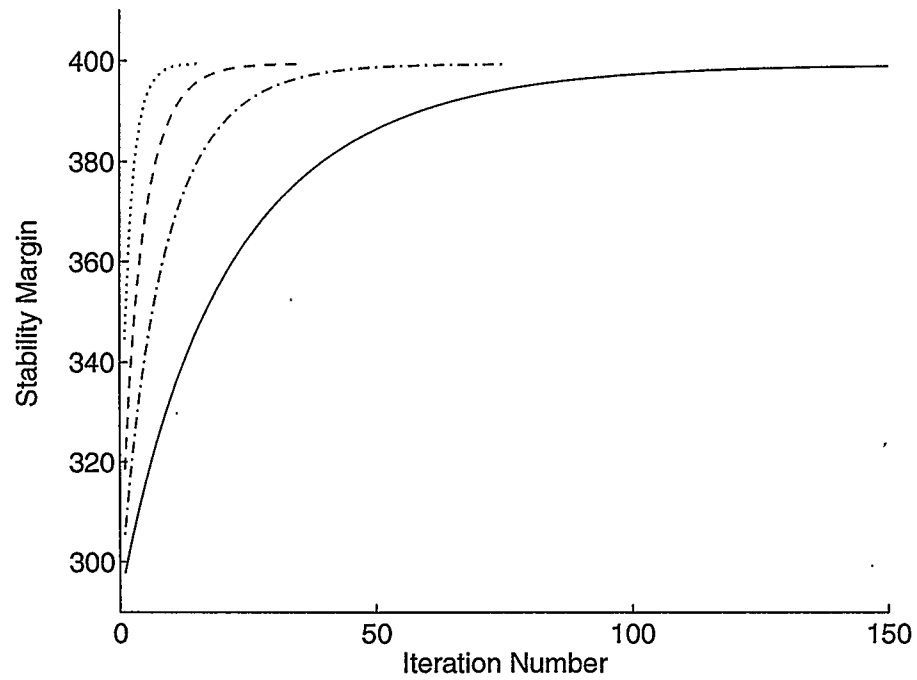


Figure 4.1: Maximum loading level versus iteration times using ICP when the desired stability margin is 400 MW. The dotted, dashed, dashdot and solid lines correspond to $\beta = 2, 1, 0.5$ and 0.2 respectively.

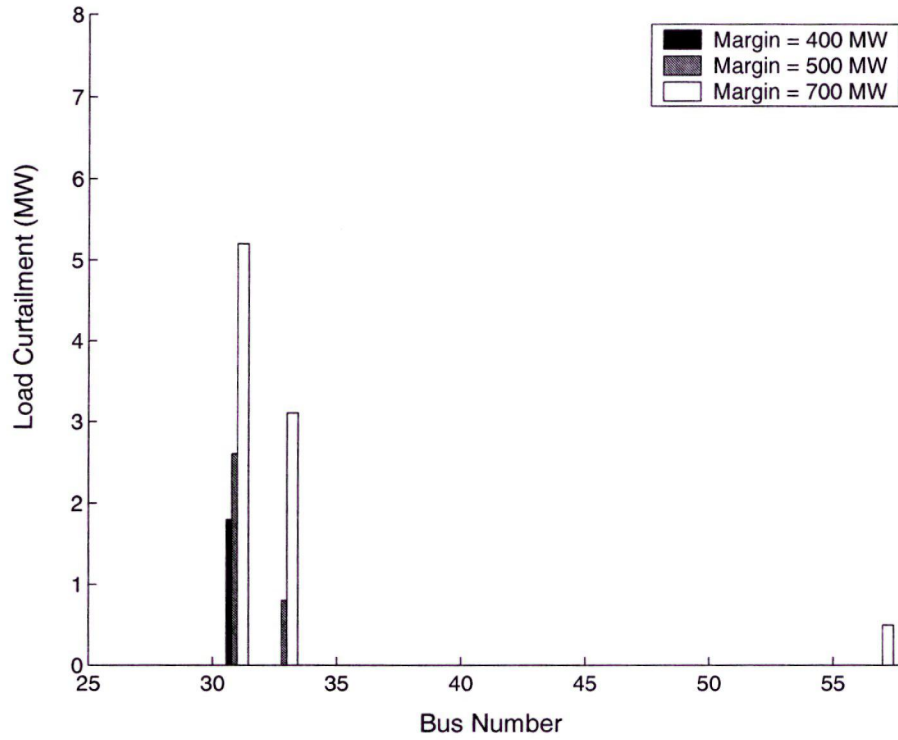


Figure 4.2: Load curtailment on each bus using ICP when the desired stability margin is 400 MW, 500 MW and 700 MW.

desired stability margin is 500 MW, the results show that bus 33 has the greatest effect in some iterations and bus 31 is no longer the only bus that should have load curtailment. Moreover, when the desired stability margin is 700 MW, bus 57 will be required to curtail some loads. This is one of the advantages of the Iterative Curtailment Procedure compared to the Single Curtailment Procedure, which only cut load once and ignore the change of Lagrange multipliers.

Figure 4.3 is a plot of the magnitude of the Lagrange multipliers at different iterations of the procedure. During the initial iterations, the effect of each of the buses on the system maximum loadability is very different, with Bus 31 having initially the greatest impact. After several iterations of the procedure, the relative

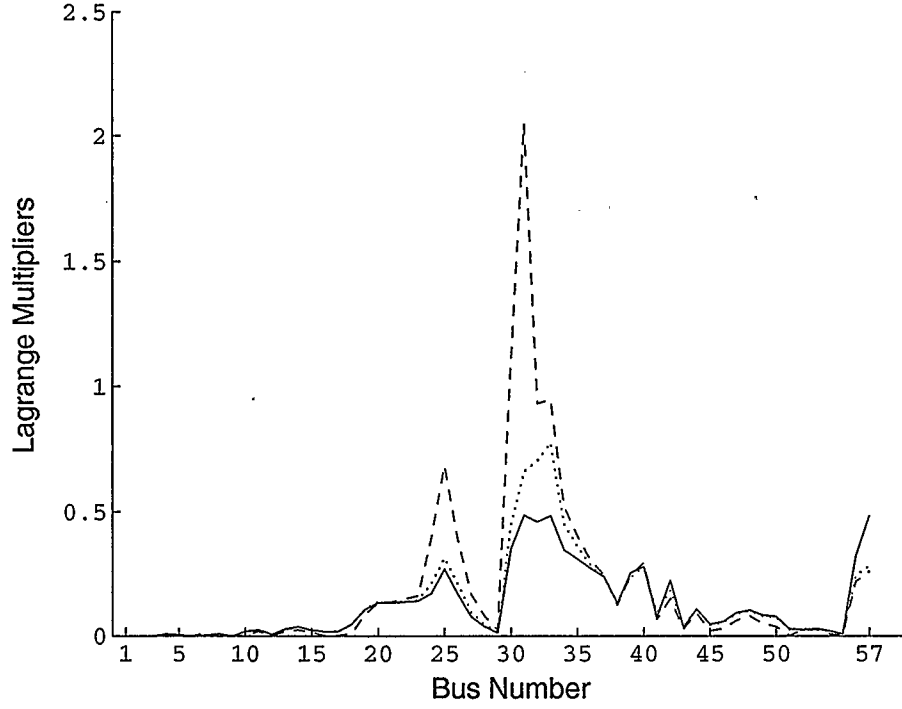


Figure 4.3: Lagrange multipliers of each bus using ICP when the desired stability margin is 700 MW. The dash, dotted and solid lines correspond to iteration times = 1, 30 and 115 respectively.

impact of each of the buses is more equal.

Figure 4.4 shows the iteration numbers while implementing the Iterative Curtailment Procedure to reach different desired stability margins. In this case, the scalar β was held constant at one. The symbol * indicates the iterations when 95% of the desired stability margins are reached. From this figure, the higher the desired stability margin, the more iteration times required.

The iterative Curtailment Procedure checks the Lagrange Multiplier every iteration, where the Single Curtailment Procedure only checks the Lagrange Multiplier at the original loading level. Therefore, the Iterative Curtailment Procedure is more accurate and preferred. However, the Iterative Curtailment Procedure takes more time

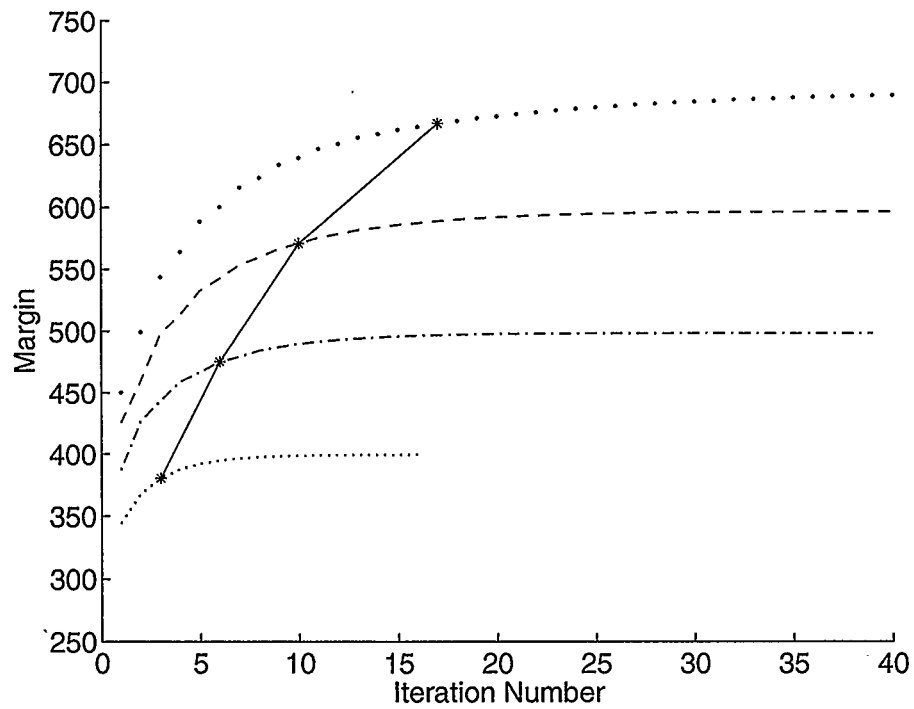


Figure 4.4: The Comparison of ICP with different stability margin. The dotted, dashdot, dashed and big dotted correspond to stability margin = 400, 500, 600 and 700 respectively. The solid line indicates when 95 % of the desired stability margin is reached.

to approach the desired maximum loading level. Moreover, the Iterative Curtailment Procedure sometimes fails to meet the desired maximum loading level because there are no loads to curtail on the bus with largest Lagrange multiplier.

4.4 Summary

This section presents an iterative and single cut approach to curtail load that is participating in a Fast Acting Load Control program. The approaches are based on using Lagrange multipliers to not only identify which buses should be selected for load curtailment but also the amount of load that should be curtailed from the buses. First order Taylor series expansions are used to explicitly find an approximate relationship between the loading level at a particular bus and the stability margin of the system. Results from applying the approaches to the IEEE 57-bus system showed that the iterative approach was better used to the load curtailment problem because of the nonlinear nature of power system models.

Chapter 5

Optimal Load Curtailment Program

5.1 Introduction

Load control in bulk power systems has been studied for many years [41]. The load control schemes to prevent power system losing stability can be classified into two sorts:

1. Improvement Based Load Control: This method determine which loads and how much load should be curtailed if the stability margin of the current operating point is lower than a desired value.
2. Contingency Based Load Control: This method analyzes the system stability margin with respect to credible contingencies, i.e. incidents with a reasonable probability of occurrence, and control loads to restore sufficient margins when needed.

A Lagrange Based Fast Acting Load Control (LB-FALC) technique is proposed in Chapter 4. The technique uses Lagrange multipliers to identify buses where loads are having the greatest impact on system stability. However, one disadvantage of using Lagrange multipliers is that they are only a local estimate. Furthermore, it tends to take a long time to approach the optimal solution, and the LB-FALC can only consider the Maximum Loadability problem. Therefore, in this chapter, an Optimal Load Curtailment (OLC) formulation is introduced to determine the location and

amount that should be curtailed to meet stability and cost requirements.

5.2 Improvement Based Load Curtailment Modelling

System load is modelled as a static load model with constant active and reactive power, which is called constant PQ load. At the present operating condition, the load model can be represented as follows:

$$\begin{aligned} \mathbf{P}_l &= \lambda_0 \mathbf{P}_0 \\ \mathbf{Q}_l &= \lambda_0 \mathbf{Q}_0 \end{aligned} \tag{5.1}$$

where $\lambda_0 \in \{\lambda_{p0}, \lambda_{*0}\}$ is used to map the base load (P_0, Q_0) to the present and critical loading levels.

When the Fast Acting Load Control is applied, the system loading level reduces. The load can be modelled as follows:

$$\begin{aligned} \mathbf{P}_l &= \lambda \mathbf{P}_{ln} \\ \mathbf{Q}_l &= \lambda \mathbf{Q}_{ln} \end{aligned}$$

where $(\mathbf{P}_{ln}, \mathbf{Q}_{ln})$ is the loading level after curtailment, $\lambda \in \{\lambda_p, \lambda_*\}$ is used to map the load $(\mathbf{P}_{ln}, \mathbf{Q}_{ln})$ to the present and critical loading levels. Since this is an improvement based approach, the load is curtailed at both the current and maximum loading points.

The system stability margin can be expressed in per unit or *MW*. When expressed in per unit, the margin can be represented as follows:

$$\lambda_m = \lambda_* - \lambda_p \tag{5.2}$$

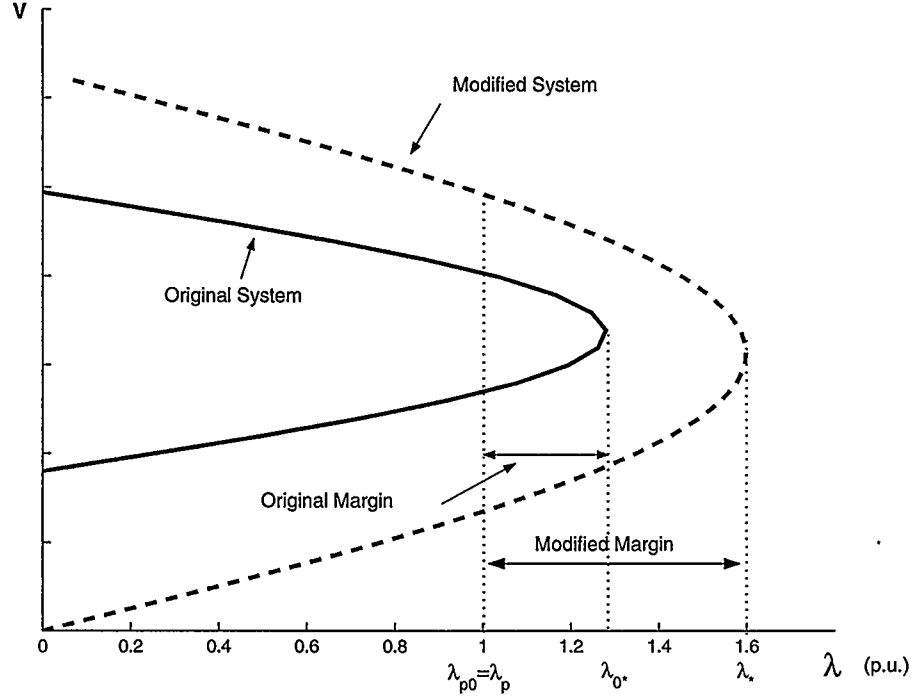


Figure 5.1: Illustration of Optimal Load Curtailment program with the stability margin in percentage. The solid and dashed lines represent the pre and after conditions of load curtailment respectively.

where λ_m represents the stability margin. In the work presented in the thesis, a power base of 100 MW is used. The present loading level parameters λ_{p0} and λ_p are equal to one before and after the load curtailment. Typical PV curves for before and after Optimal Load Curtailment are illustrated as Figure 5.1. In this figure, the stability margin is represented in per unit.

The stability margin can also be represented in MW as follows:

$$\lambda_m = P_{lt}(\lambda_* - \lambda_p) \quad (5.3)$$

where λ_m represents the stability margin and P_{lt} is summation of the active power of all the loads in the system. The present loading level parameter λ_p is in different

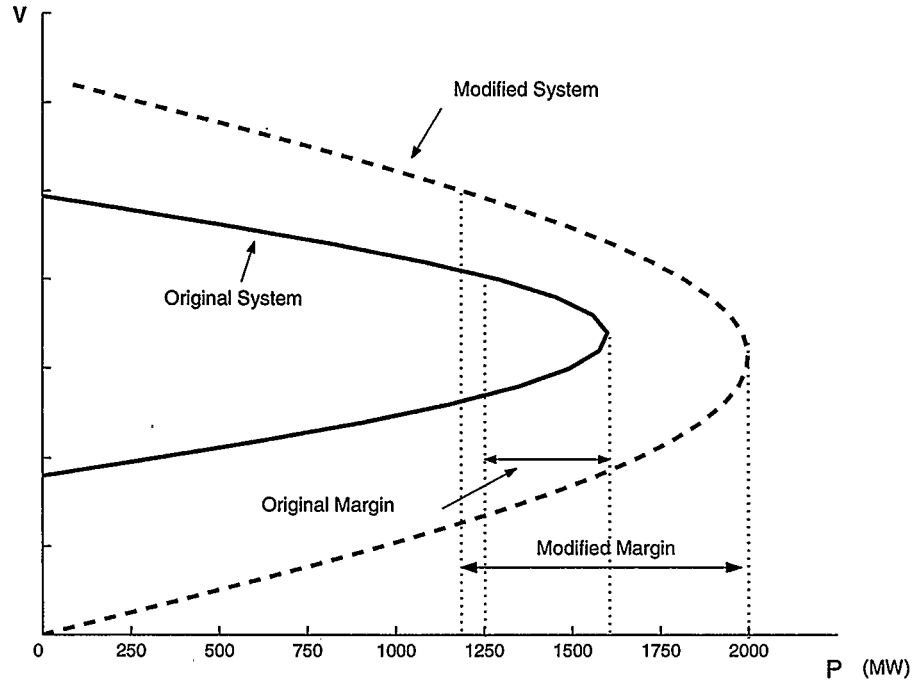


Figure 5.2: Illustration of Optimal Load Curtailment program with the stability margin in *MW*. The solid and dashed lines represent the before and after conditions of load curtailment respectively.

values in *MW* before and after the load curtailment while the total loads reduce. In Figure 5.2, the PV curves of different operation conditions are illustrated while the stability margin is represented in *MW*.

5.3 Generation Cost Minimization Optimal Power Flow

The Generation Cost Minimization Optimal Power Flow (GCM-OPF) problem can be modelled to determine generation scheduling for a pool based electricity market. The formulations can be expressed as following:

$$\begin{aligned}
\min \quad & G(\mathbf{x}_p, \boldsymbol{\rho}, \lambda_p) \\
\text{s.t. :} \quad & \mathbf{F}(\mathbf{x}_p, \boldsymbol{\rho}, \lambda_p) = \mathbf{0} \quad (\text{Load Flow Eqns.}) \\
& \mathbf{H}_T(\mathbf{x}_p, \boldsymbol{\rho}) \leq \overline{\mathbf{H}}_T \quad (\text{Transmission Line Limits}) \\
& \underline{\mathbf{H}}_B \leq \mathbf{H}_B(\mathbf{x}_p, \boldsymbol{\rho}) \quad (\text{Generator Lower Bid Limits}) \\
& \mathbf{H}_B(\mathbf{x}_p, \boldsymbol{\rho}) \leq \overline{\mathbf{H}}_B \quad (\text{Generator Upper Bid Limits}) \\
& \mathbf{H}_R(\mathbf{x}_p, \boldsymbol{\rho}) \leq \overline{\mathbf{H}}_R \quad (\text{Active Power Reserve Margin}) \\
& \underline{\mathbf{x}}_p \leq \mathbf{x}_p \leq \overline{\mathbf{x}}_p \quad (\text{Dependent Variable Limits}) \\
& \underline{\boldsymbol{\rho}} \leq \boldsymbol{\rho} \leq \overline{\boldsymbol{\rho}} \quad (\text{Independent Variable Limits})
\end{aligned} \tag{5.4}$$

where the objective function,

$$G(\mathbf{x}_p, \boldsymbol{\rho}, \lambda_p) = \sum_{i \in g} C_i P_i \tag{5.5}$$

includes the bid price \mathbf{C} for energy, which is a constant vector, and the independent variable P_i which is the amount of generation scheduled from generator i . The symbol g represents the set of generators in the system. The formulation (5.4) represents a typical Optimal Power Flow problem with generator cost minimization.

5.4 Optimal Load Curtailment

The Optimal Load Curtailment problem can be formulated as follows:

$$\begin{aligned}
& \min && P_r && (5.6) \\
& \text{s.t. :} && \mathbf{F}(\mathbf{x}_p, \boldsymbol{\rho}, \lambda_p) = \mathbf{0} \\
& && \mathbf{F}(\mathbf{x}_*, \boldsymbol{\rho}, \lambda_*) = \mathbf{0} \\
& && P_{lt}(\lambda_* - \lambda_p) \geq \lambda_{md} \\
& && \underline{\mathbf{H}} \leq \mathbf{H}(\mathbf{x}_p, \boldsymbol{\rho}) \leq \overline{\mathbf{H}} \\
& && \underline{\mathbf{H}} \leq \mathbf{H}(\mathbf{x}_*, \boldsymbol{\rho}_*) \leq \overline{\mathbf{H}}
\end{aligned}$$

where P_r is the total amount of loads curtailed, $\mathbf{F}(\mathbf{x}, \boldsymbol{\rho}, \lambda)$ functions are load flow equations, $\mathbf{H}(\mathbf{x}, \boldsymbol{\rho})$ represent the transmission line and generator active power limits, and the subscripts p and $*$ indicate the present and collapse points, respectively. To simplify the expression, the upper and lower limits of system variables \mathbf{x} and $\boldsymbol{\rho}$ are included in $\overline{\mathbf{H}}$ and $\underline{\mathbf{H}}$. P_{lt} is the total amount of loads in the system and λ_{md} is the desired stability margin expressed in *MW*.

The following inequality has been added to (5.6) to set the stability margin as a constraint:

$$P_{lt}(\lambda_* - \lambda_p) \geq \lambda_{md} \quad (5.7)$$

The objective of (5.6) is to minimize the amount of load that should be reduced. Normally, when the load is reduced, the generators will also reduce their active power production to balance the system power flow. Therefore, the generator scheduling needs to change. Based on economic operation, the generator with the highest bid should produce the least power. To consider generation cost as well as stability margin of the system, the following four techniques are proposed:

1. **Fixed Generator Scheduling Technique (FGST):** Based on a Generation Cost Minimization OPF (GCM-OPF) solution, solve the Optimal Load Curtailment problem while fixing the generator active power scheduling, except for the slack bus.
2. **Generator Active Power Distributed Technique (GAPDT):** Based on a Generation Cost Minimization OPF (GCM-OPF) solution, solve the Optimal Load Curtailment problem while distributing changes to the active power of generator according to a participation factor. The participation factor is a function of current generator active power settings, which depends on the margin to generator active power lower limit.
3. **Cost Constraint Technique (CCT):** Based on a Generation Cost Minimization OPF (GCM-OPF) solution, solve the Optimal Load Curtailment problem with a constraint that the total generation cost of the curtailed system is within a cost limit. The cost limit is based on the solution of the GCM-OPF.
4. **Multi-Objective Technique (MOT):** Based on a Generation Cost Minimization OPF (GCM-OPF) solution, introduce a new function incorporating changes of the generation settings into the objective function of Optimal Load Curtailment formulation. The motivation of Multi-Objective Technique is to meet all stability constraints with the least change of load and generation.

Generally, the Optimal Load Curtailment schemes can be illustrated with the chart in Figure 5.3. As shown in the chart, the initial values of system variables \mathbf{x}_0 and ρ_0 are firstly used as the input data for the Generation Cost Minimization

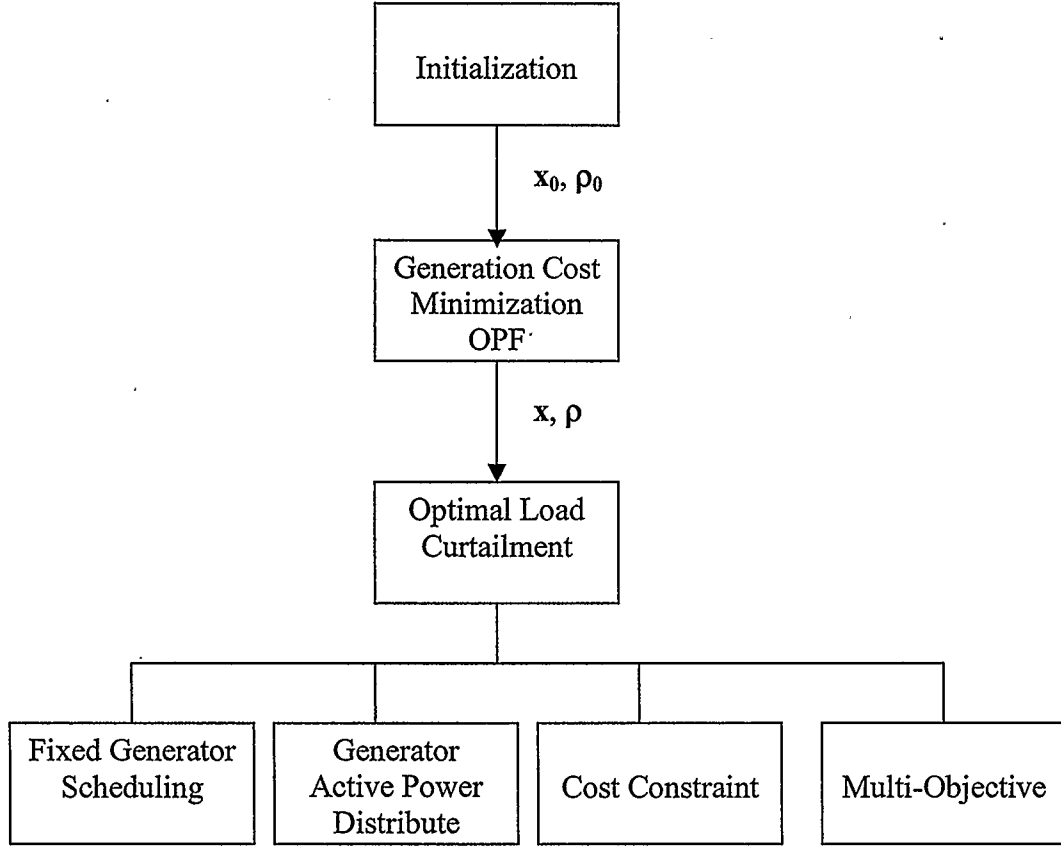


Figure 5.3: Illustration of Optimal Load Curtailment program.

OPF (GCM-OPF) formulation. And then, the solutions of GCM-OPF \mathbf{x} and $\boldsymbol{\rho}$ are loaded as the input data for the Optimal Load Curtailment formulation. The system variables including depended variables \mathbf{x} , which include voltages and angles of load buses, reactive power and angles of generator buses and independent variables $\boldsymbol{\rho}$ such as active powers of generator and load buses.

5.4.1 Fixed Generator Scheduling Technique (FGST)

The main steps in the Fixed Generator Scheduling Technique are as follows:

1. Solve the Generation Cost Minimization Optimal Power Flow (GCM-OPF)

problem formulated in (5.4).

2. Set the solutions of step # 1 as the input of Optimal Load Curtailment program.
3. Solve the Optimal Load Curtailment formulation 5.6 while fixing the generator active power scheduling from the solution of step # 1, except for the slack bus.

Sometimes, when active power is fixed at generator buses except for the slack bus, there will be no convergence of the OLC program. This is because there could be no room for reduction when loads are removed to balance the load flow equations. To solve this potential unconvergence problem, active power of slack bus is set free, and is set a negative lower limit. However, having the active power of the slack bus being negative is not practical.

Changing the slack bus is considered when the active power at slack bus goes negative. Normally, the slack bus should have enough active and reactive power to balance the whole system.

5.4.2 Generator Active Power Distributed Technique (GAPDT)

The main steps in the Generator Active Power Distributed Technique are as follows:

1. Solve the Generation Cost Minimization Optimal Power Flow (GCM-OPF) problem formulated in (5.4).
2. Set solutions of step # 1 as the input of the Optimal Load Curtailment program.

3. Introduce the participation parameter $\mu[i]$ and the distribution parameter ν , so that reductions in the generator's active power is distributed as follows:

$$P_g[i] = P_{g0}[i] - \mu[i] * \nu \quad (5.8)$$

where $i \in gb$, and gb is the set of generator buses in the system, $\mu[i]$ is the participation factor and ν is the distribution parameter. The participation factor $\mu[i]$, a function of current generator active power settings, depends on the margin to the generator lower active power limit. For example, if the generator at bus 5 is at a lower limit, then $\mu[5]$ is set to zero.

Adding (5.8) as a constraint into formulation (5.6), the GAPDT problem can be written as:

$$\begin{aligned} \min \quad & P_r \quad (5.9) \\ \text{s.t. :} \quad & \mathbf{F}(\mathbf{x}_p, \boldsymbol{\rho}, \lambda_p) = \mathbf{0} \\ & \mathbf{F}(\mathbf{x}_*, \boldsymbol{\rho}, \lambda_*) = \mathbf{0} \\ & P_{lt}(\lambda_* - \lambda_p) \geq \lambda_{md} \\ & P_g[i] = P_{g0}[i] - \mu[i] * \nu \quad \forall i \in gb \\ & \underline{\mathbf{H}} \leq \mathbf{H}(\mathbf{x}_p, \boldsymbol{\rho}) \leq \overline{\mathbf{H}} \\ & \underline{\mathbf{H}} \leq \mathbf{H}(\mathbf{x}_*, \boldsymbol{\rho}_*) \leq \overline{\mathbf{H}} \end{aligned}$$

where gb is the set of generator buses in the system, \mathbf{x}_0 and $\boldsymbol{\rho}_0$ are system depended and independed variables.

4. Solve the new Optimal Load Curtailment problem (5.9) with the generator active power distributed.

5.4.3 Cost Constraint Technique (CCT)

The main steps in the Cost Constraint Technique are as follows:

1. Solve the Generation Cost Minimization Optimal Power Flow (GCM-OPF) problem formulated in (5.4).
2. Based on the Optimal Load Curtailment formulation (5.6), the following inequality relating to generation cost is added as a constraint:

$$C_g \leq \overline{C} \quad (5.10)$$

where the cost limit \overline{C} can be defined as follows:

$$\overline{C} = \beta_c C_0 \quad (5.11)$$

where $0 \leq \beta_c \leq 1$ is a scalar used to control the total cost limit, and C_0 is the generation cost by solving generator operation cost minimization Optimal Power Flow (OPF) problem at the original loading level. The load curtailment always tends to reduce the generation production, and the generation operation cost should decrease after load curtailment, so the parameter β_c tends to be equal or less than one to incorporate this effect. The new Optimal Load

Curtailment problem can be written as:

$$\begin{aligned}
 & \min && P_r && (5.12) \\
 & \text{s.t. :} && \mathbf{F}(\mathbf{x}_p, \boldsymbol{\rho}, \lambda_p) = \mathbf{0} \\
 & && \mathbf{F}(\mathbf{x}_*, \boldsymbol{\rho}, \lambda_*) = \mathbf{0} \\
 & && P_{lt}(\lambda_* - \lambda_p) \geq \lambda_{md} \\
 & && C_g \leq \overline{C} \\
 & && \underline{\mathbf{H}} \leq \mathbf{H}(\mathbf{x}_p, \boldsymbol{\rho}) \leq \overline{\mathbf{H}} \\
 & && \underline{\mathbf{H}} \leq \mathbf{H}(\mathbf{x}_*, \boldsymbol{\rho}_*) \leq \overline{\mathbf{H}}
 \end{aligned}$$

3. Solve the new Optimal Load Curtailment problem 5.12 with the cost constraint.

In this technique, active power on generator buses is not fixed, and the generator cost is considered as a constraint. However, this formulation only considers loads, not generators in the objective, so that would tend to have generators be rescheduled more than loads, except for the new constraint. That means active power of generators are going to be rearranged while the loads are reduced, and the new generator scheduling may not meet the requirement of minimizing generator costs.

5.4.4 Multi-Objective Technique (MOT)

The main steps in the Multi-Objective Technique are as follows:

1. Solve Generation Cost Minimization Optimal Power Flow (GCM-OPF) problem formulated in (5.4).
2. Set solutions of step # 1 as the input of Optimal Load Curtailment program.

3. Introduce a new component into the objective of the formulation 5.6 to model generator operation cost as follows:

$$f(\tau, \mathbf{P}_{gr}) = \sum_{i=1}^{gb} \frac{\tau_c - \tau[i]}{\tau[i]} P_{gr}[i] \quad (5.13)$$

where $i \in gb$, gb is the set of generator buses in the system, τ_c is the clearing price of the system, $\tau[i]$ is the bid price of the i^{th} generator and $P_{gr}[i]$ is the reduction of generator active power due to curtailed loads on the i^{th} bus. Equation 5.13 is related to the generation cost function, and tends to reduce the generator active power based on cost.

The new formulation with the multiple objectives can be written as follows:

$$\min \quad \omega_1 P_r + \omega_2 f(\tau, \mathbf{P}_{gr}) \quad (5.14)$$

$$\text{s.t. :} \quad \mathbf{F}(\mathbf{x}_p, \boldsymbol{\rho}, \lambda_p) = \mathbf{0}$$

$$\mathbf{F}(\mathbf{x}_*, \boldsymbol{\rho}, \lambda_*) = \mathbf{0}$$

$$P_{lt}(\lambda_* - \lambda_p) \geq \lambda_{md}$$

$$\omega_1 + \omega_2 = 1$$

$$\underline{\mathbf{H}} \leq \mathbf{H}(\mathbf{x}_p, \boldsymbol{\rho}) \leq \overline{\mathbf{H}}$$

$$\underline{\mathbf{H}} \leq \mathbf{H}(\mathbf{x}_*, \boldsymbol{\rho}_*) \leq \overline{\mathbf{H}}$$

where $f(\tau, \mathbf{P}_{gr})$ is defined in equation (5.13), ω_1 and ω_2 are weighting factors.

4. Solve the new multiple objective Optimal Load Curtailment problem.

The purpose of weighting factors ω_1 and ω_2 is to change the emphasis placed on load curtailed versus generator operation cost. However, the exact effect of weights is not known in advance, but the general characteristics are clear.

5.5 Numerical Analysis

The Optimal Load Curtailment formulations presented above are tested on two sample systems, one based on the IEEE 30-bus test system, and the second one based on IEEE 57-bus test system [40]. The optimization problems are solved using the software package LOQO [19] and the modelling language AMPL [17].

5.5.1 Fixed Generator Scheduling Technique (FGST)

Fixing the generator scheduling based on the Generation Cost Minimization OPF results in reducing the active power at the slack bus. Sometimes the slack bus has the highest operation cost, so the active power scheduled to the slack bus is very low. When the slack bus has to reduce a lot of active power to balance the system power flow, the active power at slack bus goes negative. Having a generator bus with negative active power is not practical and leads to unconvergence in simulations. Changing the slack bus based on the original scheduling is tested on IEEE 30-bus test system.

Bus Number	Bid Price	Scheduled P_g (MW)
1	5.00	0.00
2	1.20	14.43
5	1.30	0.00
8	1.20	51.77
11	1.00	147.94
13	1.10	85.01

Table 5.1: The generator scheduling based on generator cost minimization OPF of IEEE 30-Bus System.

Table 5.1 shows the generator bid prices and scheduling after solving the generation cost minimization OPF problem of IEEE 30-Bus test system. When the desired

stability margin is 170 MW, the results of solving the Fixed Generator Scheduling problem with different slack bus is shown in Table 5.2 shows. Because the generator buses 1, 2 and 5 do not have enough active power to reduce when the desired stability margin is 170 MW, the simulations of choosing them as slack bus, does not converge.

Slack Bus	P_g reduced (MW)
1	No convergence
2	No convergence
5	No convergence
8	47.19
11	28.83
13	41.78

Table 5.2: The generator active power reduced when the system choosing different slack bus.

When using this approach, the slack bus should be the one that has the most generator active power. Figure 5.4 depicts the curtailed amount of loads at different desired stability margins when choosing a different slack bus. Different generator buses have different effects for the system stability, so choosing different slack bus may result in a different amount of load curtailment. From the observation of Figure 5.4, Bus 11 is better suited to be set for the slack bus because of the reduced curtailment.

Figure 5.5 illustrates the total generation cost at different desired stability margins when a different slack bus is chosen. Because of the load curtailment, generators tend to reduce the production to balance the system power flow, which leads to the decreasing generation cost when increasing the desired stability margin.

Based on the Generation Cost Minimization OPF, cheaper generator tends to have more generation production. Choosing the bus that has the most active power

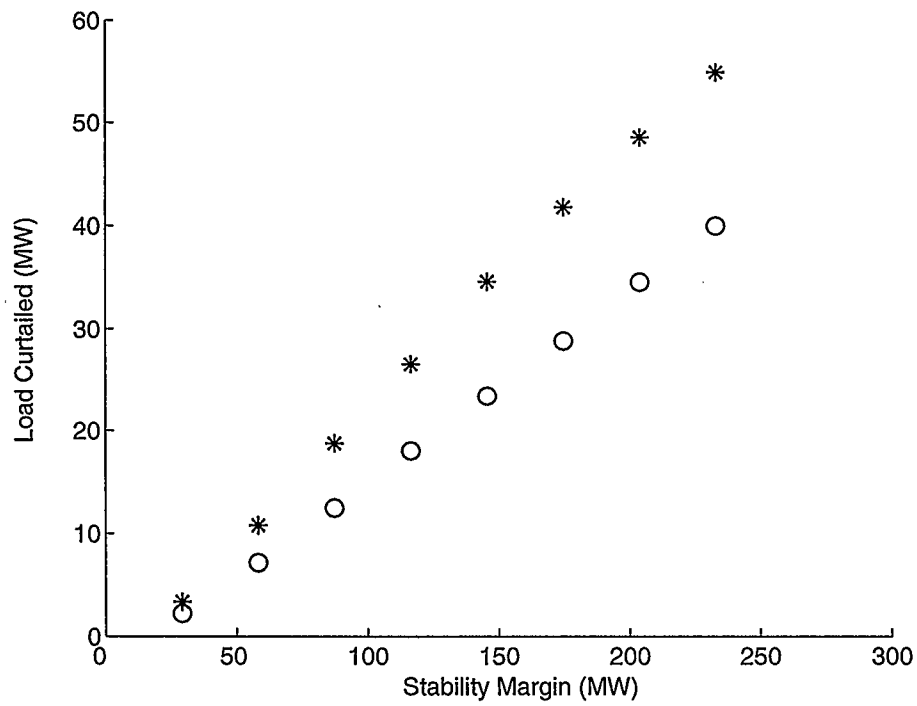


Figure 5.4: Load curtailment versus stability margin using Fixed Generator Scheduling technique with different slack bus. The symbols \circ and $*$ correspond to solutions for the system choosing # 11 and # 13 bus as slack bus respectively.

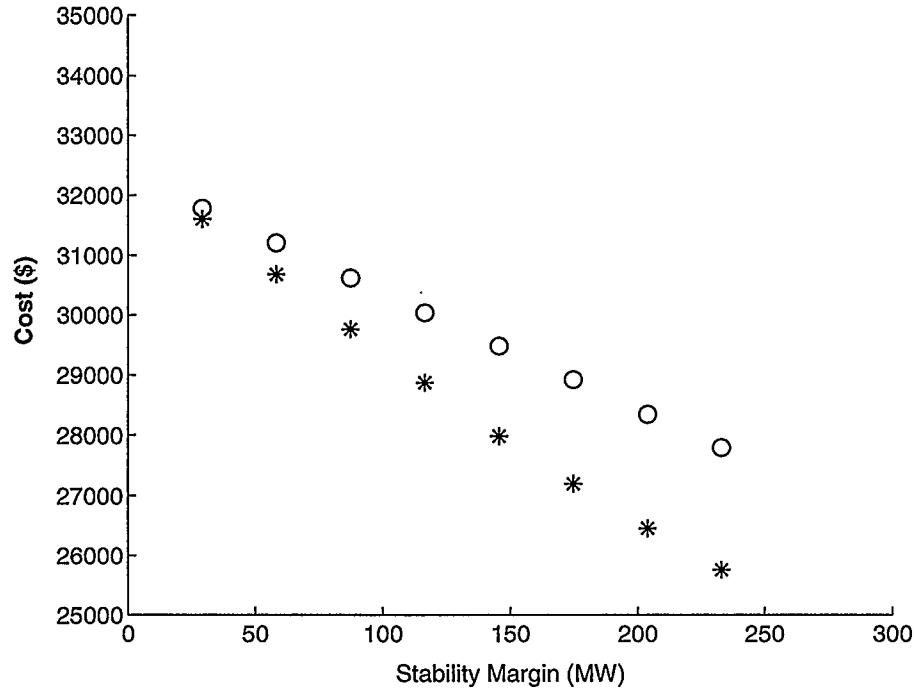


Figure 5.5: Total generator cost versus stability margin using Fixed Generator Scheduling technique with different slack bus. The symbols o and * correspond to solutions for the system choosing # 11 and # 13 bus as slack bus respectively.

as slack bus is not always positive for generator cost minimization. In the case shown in Figure 5.4, less load curtailment leads to less generator reduction, and then tends to result in more generation cost. This disadvantage of choosing Bus 11 as the slack bus is depicted in Figure 5.5 where the total generator cost is higher when selecting Bus 11 as the slack bus. However, because the loads can also bid for curtailment, the less load curtailment tends to results in the less payment for the loads curtailed. Therefore, when changing the slack bus is necessary, the generator bus having the most active power in the original scheduling is chosen as the new slack bus.

5.5.2 Generator Active Power Distributed Technique (GAPDT)

The Generator Active Power Distributed Technique (GAPDT) is then applied to IEEE 30-Bus test system. This technique balances the system power flow by distributing the reduction in generator active power between all generator buses.

Figure 5.6 illustrates the amount of loads that should be curtailed to meet different desired stability margins. The advantage in minimizing the load curtailment using Generator Active Power Distributed Technique can be observed in the figure. The Generator Active Power Distributed Technique (GAPDT) results in less load curtailment compared to Fixed Generator Scheduling Technique (FGST). In the Fixed Generator Scheduling Technique, the generator scheduling is fixed except for the slack bus, so only one generator bus is available to balance the whole system power flow. However, in the Generator Active Power Distributed Technique, all the generator buses are controllable based on the participation parameters. Because the reduction in generation can be distributed between all the generator buses in GAPDT, it is possible to find a better solution for minimizing the amount of load curtailment.

5.5.3 Cost Constraint Technique (CCT)

Next, a set of numerical analysis was performed applying the Cost Constraint Technique (CCT) to IEEE 57-Bus test system. Unlike the Fixed Generator Scheduling Technique and the Generator Active Power Distributed Technique, the generator scheduling based on the generation cost minimization OPF is free to vary. Instead, a total generation cost limit is set as a constraint in this technique. The cost limit is based on the solution of generation cost minimization OPF, but a control parameter

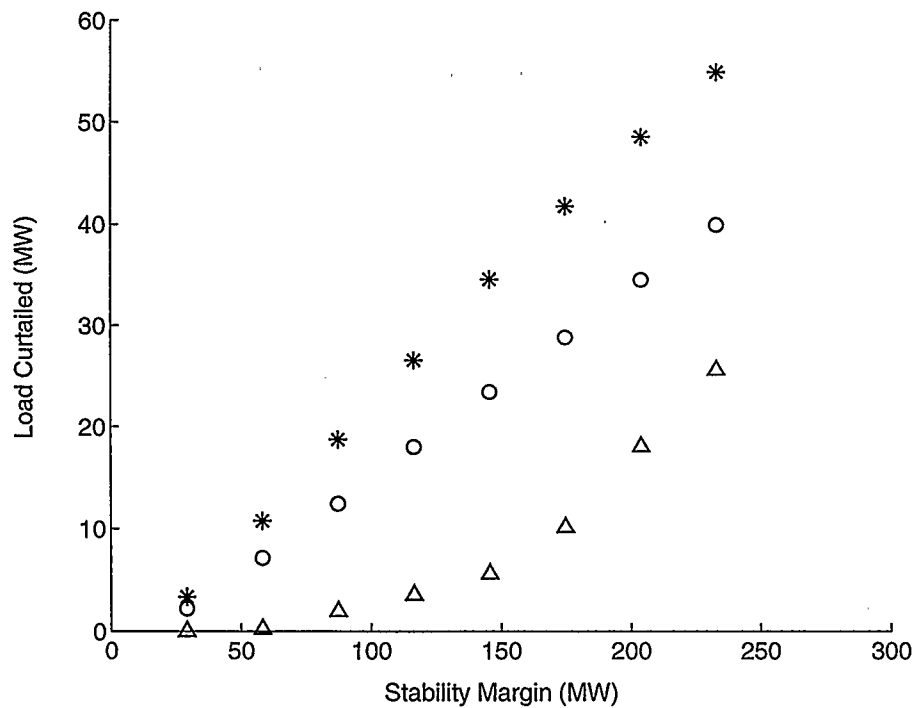


Figure 5.6: Load curtailment versus stability margin using the Generator Active Power Distributed technique and Fixed Generator Scheduling technique with different slack buses. The symbols Δ , \circ and $*$ correspond to solutions for the system using the Generator Active Power Distributed technique, Fixed Generator Scheduling technique choosing # 11 as slack bus and Fixed Generator Scheduling technique choosing # 13 bus as slack bus respectively.

β_c is incorporated. The parameter β_c is a scalar between zero and one. However, if β_c is chosen too low, the system may curtail more loads to meet the generation cost constraint. Figure 5.7 shows the load curtailment results using different values of parameter β_c .

Generally, the stability constraint, $\lambda_* - \lambda_p \geq \lambda_m$, has an effect on the objective function, which means the higher the stability margin, the more loads tends to be curtailed. However, when β_c is less than one and the desired stability margin is low, the cost constraint, $C_g \leq \beta_c C_0$, tends to have more effect on the objective function. In other words, when the cost limit is low, the system has to curtail more loads to meet the cost requirement. It can be observed from Figure 5.7 that when the desired stability margin is 250 MW, the amounts of load should be curtailed are 11 MW and 23 MW when β_c is chosen as 0.99 and 0.98 respectively. However, when β_c is equal to one, the amount of load should be curtailed is zero to reach the stability margin 200 MW.

To avoid the excessive load curtailment due to the cost limit, the value of parameter β_c is always set equal to one.

5.5.4 Multi-Objective Technique (MOT)

The final set of numerical analysis is applying the Multi-Objective Technique (MOT) to the IEEE 57-Bus test system. Figure 5.8 depicts the load curtailed versus stability margin when using different values of weighting factors.

It is observed that the amount of load curtailed is greater when choosing ω_1 smaller. In other words, when less emphasis is laid on load curtailment, more loads need to be curtailed to meet the stability requirement. However, the effects of differ-

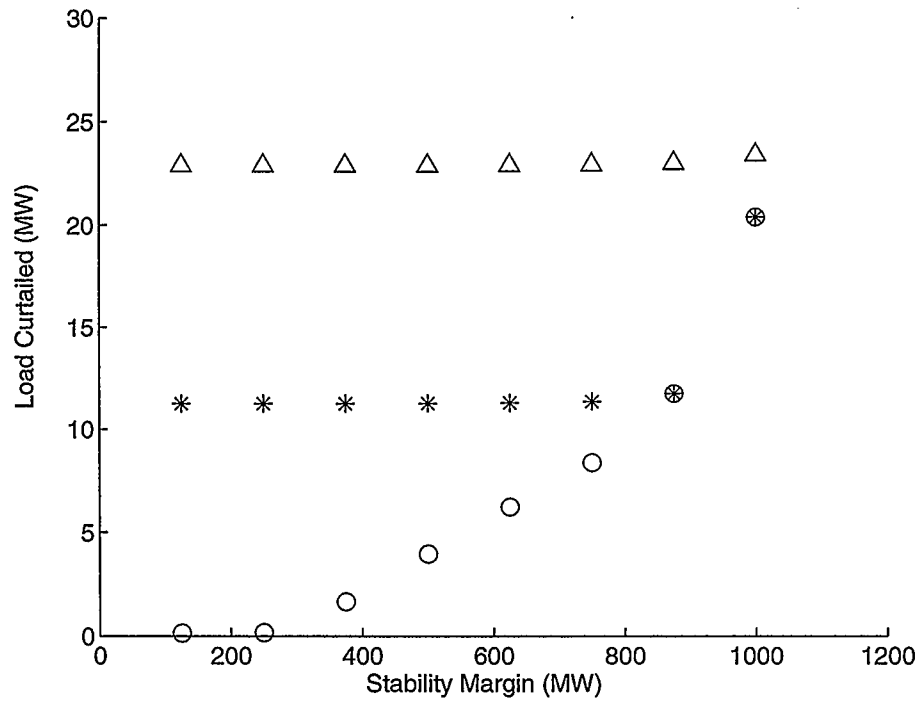


Figure 5.7: Load curtailment versus stability margin using different cost control parameter β in Cost Constraint technique to IEEE 57-Bus test system. The symbols o, * and \triangle correspond to solutions by using $\beta_c = 1, 0.99$ and 0.98 respectively.

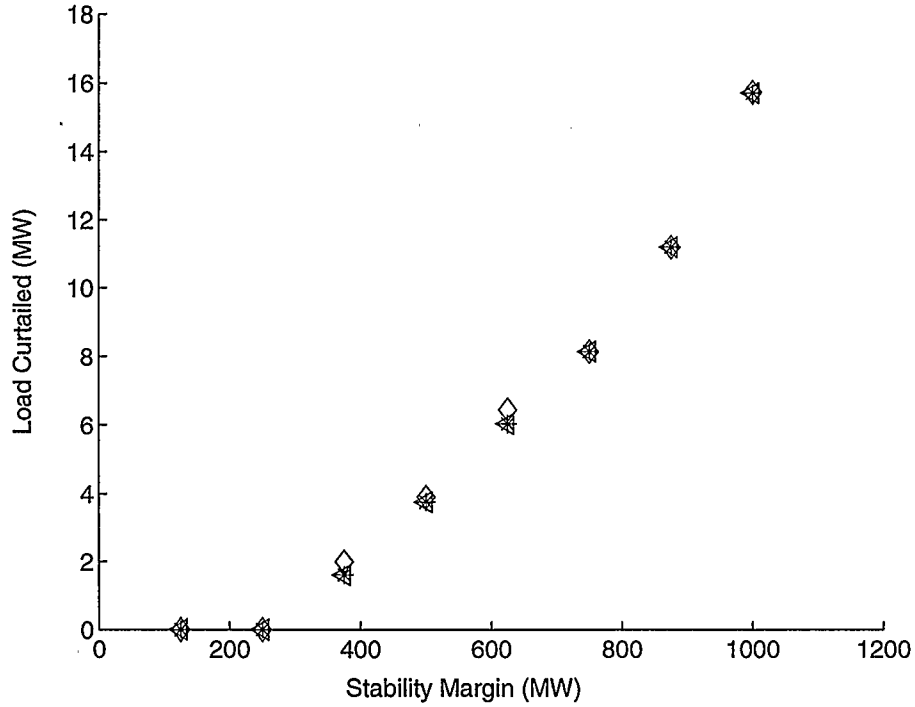


Figure 5.8: Load curtailment versus stability margin using different weighting factors in Multi-Objective Technique to IEEE 57-Bus test system. The symbols *, \triangleleft and \diamond correspond to solutions by using $\omega_1 = 0.99$, 0.5 and 0.001 respectively.

ent weighting factors are not very obvious, which is because the load curtailment and the reduction of generation cost are not always conflicting each other. Normally, the load flow equations give the relationship of the load curtailment and the reduction of generation. Therefore, different weighting factors do not have conspicuous effects on the results.

In Figure 5.9, the generation cost versus stability margin using different weighting factors is illustrated. From the figure, it is also observed that the cost is only affected a little by the changes in the weighting factors.

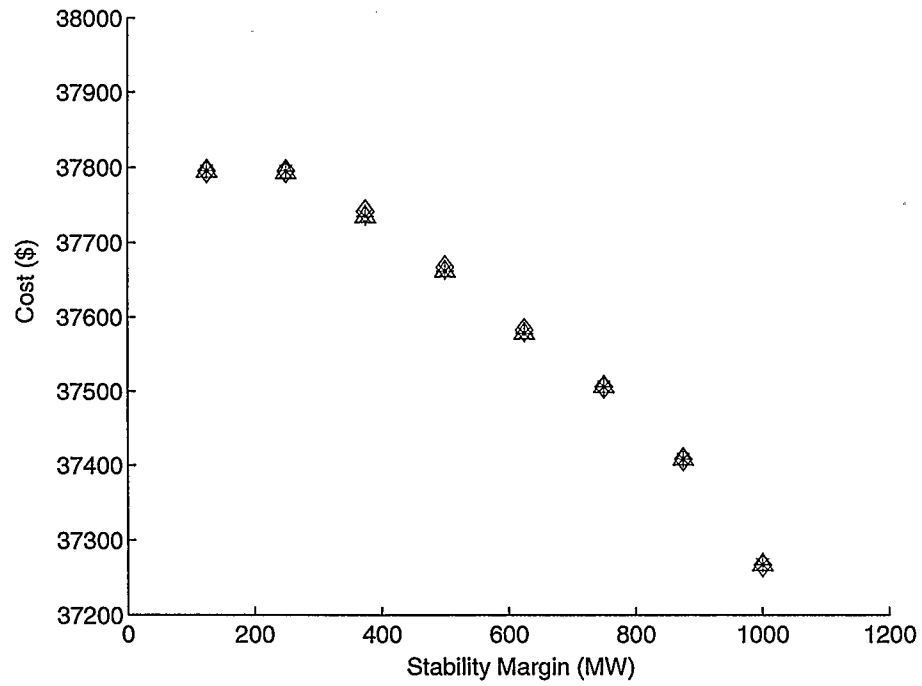


Figure 5.9: Cost versus stability margin using different weighting factors in Multi-Objective Technique to IEEE 57-Bus test system. The symbols *, ◄ and ◊ correspond to solutions by using $\omega_1 = 0.99, 0.5$ and 0.001 respectively.

5.5.5 Comparison of Results

Comparison of four techniques

To generally compare the results from the four technique proposed in section 5.4, Figure 5.10 illustrates the load curtailment versus stability margin results. Observed from the figure, the Generator Active Power Distributed, the Cost Constraint and the Multi-Objective techniques result in very similar amount of load curtailment, and Fixed Generator Scheduling technique results in the most load curtailment. Unlike the Fixed Generator Scheduling, the Generator Active Power Distributed, the Cost Constraint and the Multi-Objective techniques have all the generator buses controllable, and the generator settings are rearranged with some new constraints at the new loading level. Therefore, the Fixed Generator Scheduling technique has the highest load curtailment because the generator scheduling is fixed except for the slack bus in this technique.

The total generation cost for the different techniques is shown in Figure 5.11, which indicates that the Multi-Objective Technique (MOT) leads to the lowest generation cost and the Cost Constraint Technique (CCT) results in the highest generation cost. The Multi-Objective Technique has the objective with a generation cost component, which reduces more generater production on the bus with more expensive generator. Therefore, the MOT tends to result in the lowest generation cost. However, in the Cost Constraint Technique (CCT), the original generator scheduling is free to be rescheduled when implementing load curtailment, and the new generator scheduling may not be based on generation cost minimization. So the CCT tends to result in the highest generation cost.

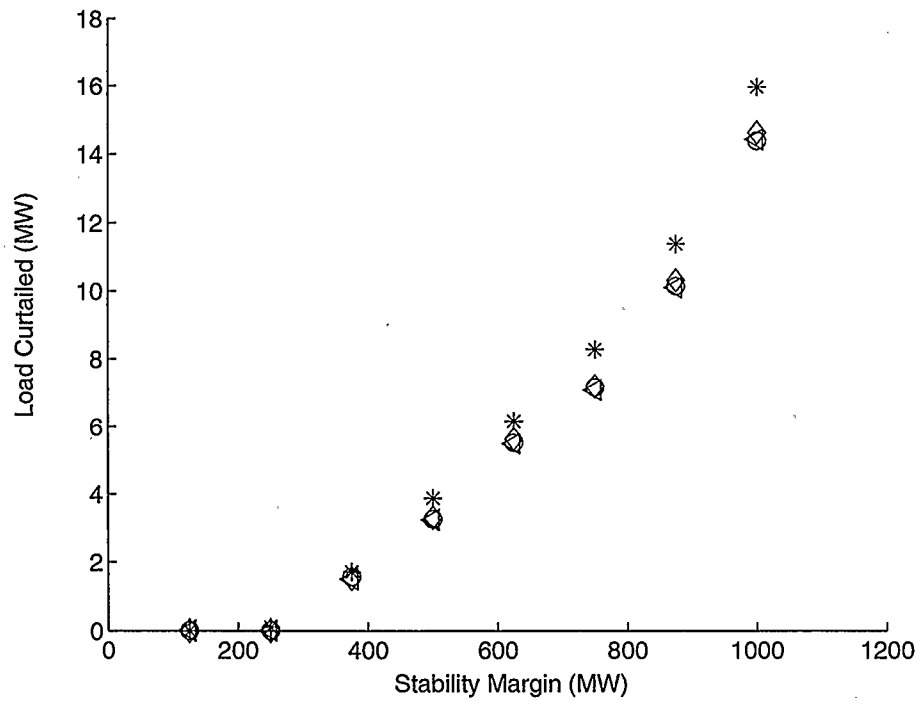


Figure 5.10: Load curtailment versus stability margin using different techniques to IEEE 57-Bus test system. The symbols *, ◇, o and ◁ correspond to solutions by using Fixed Generator Scheduling, Generator Active Power Distributed, Cost Constraint and Multi-Objective techniques respectively.

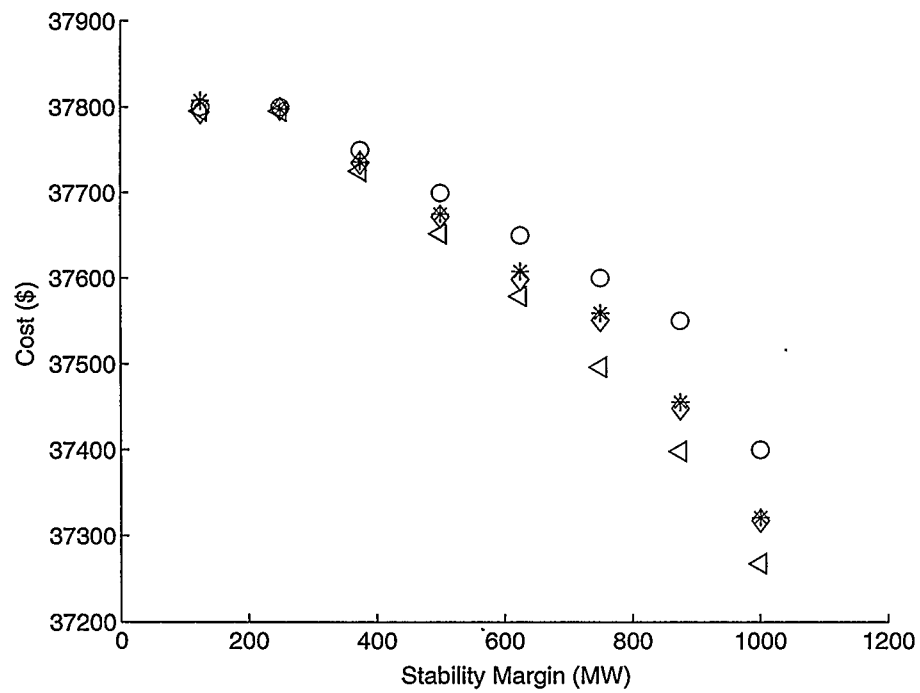


Figure 5.11: Cost versus stability margin using different techniques to IEEE 57-Bus test system. The symbols *, ◇, ○ and ◁ correspond to solutions by using Fixed Generator Scheduling, Generator Active Power Distributed, Cost Constraint and Multi-Objective techniques respectively.

Furthermore, the following tables help summarize the comparison of the four techniques.

Table 5.3 lists the amount of loads that should be curtailed based on the solutions of the four techniques presented. The results are from implementing the four techniques into the IEEE 57-Bus test system, which has the original total loads $1250.8MW$. The desired stability margin is chosen $1000MW$ in this comparison. The Cost Constraint Technique (CCT) and Multi-Objective Technique (MOT) curtail the least loads among all four techniques.

Total Loads (MW)	Curtailed Loads (MW)			
	FGST	GAPDT	CCT	MOT
1250.8	15.88	14.86	14.83	14.84

Table 5.3: The amount of total load in original system and the load curtailed to reach the stability margin $1000 MW$ by implementing FGAPT, CCT, GAPDT and MOT to IEEE 57-Bus System

Table 5.4 lists the changes in the active power settings of the generators based on the solutions of applying the four techniques into the IEEE 57-Bus test system. The total scheduled generation of the original system is $1259.8MW$. It can be observed in that the Multi-Objective Technique (MOT) changes the least generator production among all four techniques.

Total P_g (MW)	Generation Reduction (MW)			
	FGST	GAPDT	CCT	MOT
1259.8	17.42	17.15	18.62	17.05

Table 5.4: The amount of total generator active power in original system and the generation reduction to reach the stability margin $1000 MW$ by implementing FGAPT, CCT, GAPDT and MOT to IEEE 57-Bus System

Table 5.5 lists the changes in the total generator operation cost based on the

solutions of implementing the four techniques into the IEEE 57-Bus test system. As indicated in the table, the Multi-Objective Technique (MOT) results in the lowest generator operation cost.

	FGST	GAPDT	CCT	MOT
Generator Cost (\$)	37382	37329	37412	37268

Table 5.5: The generator cost after curtailing loads to reach the stability margin 1000 MW by the applying FGAPT, CCT, GAPDT and MOT to IEEE 57-Bus System

Comparison with Lagrange Based Fast Acting Load Control

A comparison of the Optimal Load Curtailment (OLC) program with the Lagrange Based Fast Acting Load Control (LB-FALC) presented in Chapter 4 is given to evaluated the advantages of direct optimization versus using lagrange multipliers.

Figure 5.12 shows the load curtailment results for different desired stability margins using the different techniques applied to the IEEE 57-Bus test system. The results of implementing Fixed Generator Scheduling, Generator Active Power Distributed, Cost Constraint and Multi-Objective techniques are represented by the symbols *, \diamond , \circ and \triangleleft respectively. The solution of Iterative Curtailment Procedure of LB-FALC is represented by the dotted line. It can be observed that the results of load curtailment by using the Generator Active Power Distributed, Cost Constraint and Multi-Objective techniques of OLC are similar with the result by using the Iterative Curtailment Procedure of LB-FALC. Therefore, the Optimal Load Curtailment (OLC) program and the Lagrange Based Fast Acting Load Control (LB-FALC) tend to obtain very similar results on the amount of load that should be curtailed to reach the desired stability margin. However, the Iterative Curtailment Procedure (ICP) of the LB-FALC takes significantly longer to approach the solution, so the Optimal

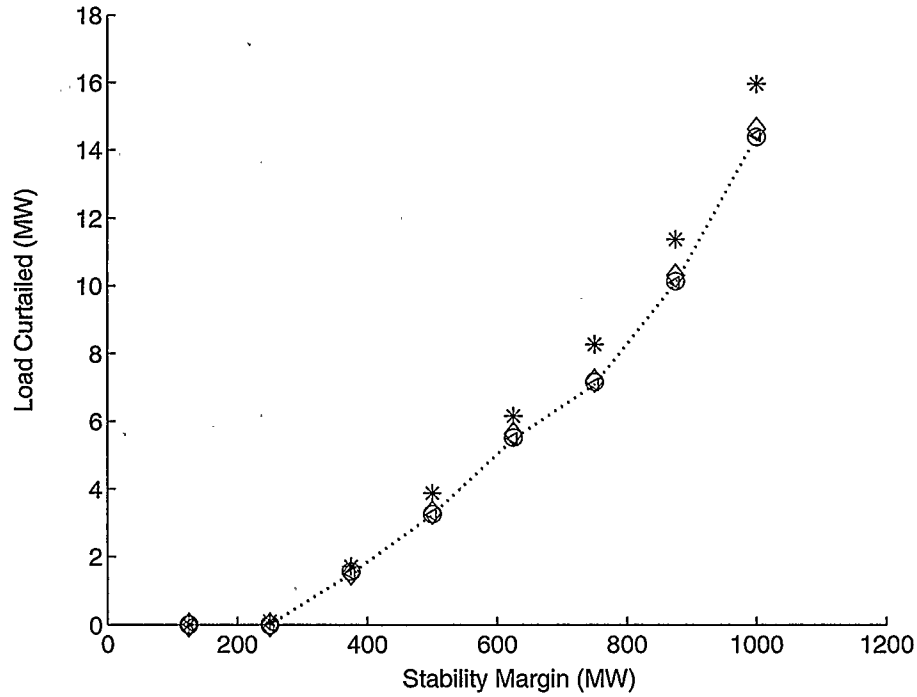


Figure 5.12: Load curtailment versus stability margin using different techniques to IEEE 57-Bus test system. The symbols *, ◇, ○ and < correspond to solutions by using Fixed Generator Scheduling, Generator Active Power Distributed, Cost Constraint and Multi-Objective techniques respectively. The dotted line represents the solution by using Iterative Curtailment Procedure of LB-FALC.

Load Curtailment program tends to be more effective on fast calculation for large systems.

5.6 Summary of Results

This chapter presents the Fixed Generator Scheduling, Generator Active Power Distributed, Cost Constraint and Multi-Objective techniques to curtail load that is participating in a Fast Acting Load Control program. The approaches are based on combining the Generation Cost Minimization OPF (GCM-OPF) and Optimal

Load Curtailment (OLC) programs to not only identify the location and amount of loads that should be selected for load curtailment but also the changes in generator scheduling that should be rearranged due to load curtailment.

The Fixed Generator Scheduling Technique (FGST) keeps the original generator scheduling except for the slack bus, but it is a challenge to change the slack bus when the original slack bus can not reduce enough active power.

The Generator Active Power Distributed Technique (GAPDT) is based on Fixed Generator Scheduling Technique, but the reduction of generation due to curtailed loads is distributed between all generator buses.

The Cost Constraint Technique (CCT) tends to result in the least load curtailment, but it also leads to the highest generation cost because of generator rescheduling. Moreover, the total generation cost limit is unknown at the beginning of the optimization analysis.

The Multi-Objective Technique (MOT) combines loads and generation cost into the objective function, and the simulation results show that this technique tends to be the best suited when considering the load curtailment and generation cost together.

The four techniques are implementing on the IEEE 30-Bus and 57-bus test systems and a comparison of results is given. It is shown that these four Optimal Load Curtailment techniques can be used to support the optimal decision making for load control and generation scheduling.

Chapter 6

Conclusions

In Chapter 2, a review of power system stability is given. Small signal stability and bifurcation analysis are introduced to analyze the system stability. Based on these bifurcation analysis methods, a Maximum Loadability problem is formulated by introducing optimization techniques.

In Chapter 3, concepts of optimization analysis are described. Lagrange methods are introduced to solve the constrained optimization problems. This is followed by the interpretation of Lagrange multipliers for the sensitivity analysis. Next, a brief review of Interior Point methods for non-linear optimization problems is presented, where the Primal-Dual Interior Point methods are used in software package LOQO to solve the optimization problems presented in this thesis.

A Lagrange Based Fast Acting Load Control (LB-FALC) procedure is presented in Chapter 4. This procedure is based on using Lagrange multipliers to identify which buses should be selected for load curtailment and the amount of load that should be curtailed from the buses. Two Lagrange based techniques, the Single curtailment and the Iterative Curtailment technique, are presented in this chapter.

Finally, in Chapter 5, an Optimal Load Curtailment procedure is proposed. This procedure considers not only the system voltage stability, but also the generator costs. Four different techniques for Optimal Load Curtailment are formulated and the simulation results are compared.

The main contributions of the thesis can be summarized as follows:

Two procedures, Lagrange Based Fast Acting Load Control (LB-FALC) and Optimal Load Curtailment (OLC), are proposed to curtail load that is participating in a Fast Acting Load Control program. Both procedures can be used to determine the optimal locations and curtailment levels for desired stability requirements. Therefore, the two load curtailment schemes tend to offer decision making support for system operators when load control is used to enhance power system stability.

Appendix A

List of Acronyms and Symbols

DAE	Differential-Algebraic Equations
FALC	Fast Acting Load Control
IEEE	Institute of Electrical and Electronics Engineers
IPM	Interior Point Method
KKT	Karush Kuhn Tucker
LM	Lagrange Multiplier
LB-FALC	Lagrange Based Fast Acting Load Control
ML	Maximum Loadability
NLP	Non-linear Programming
OLC	Optimal Load Curtailment
OPF	Optimal Power Flow
P	Real Power
PDIPM	Primal-Dual Interior-Point Method
p.u.	Per unit
Q	Reactive power
V	Voltage
η	Eigenvalues
δ	Angular position of rotor
ω	Angular velocity of rotor
\mathbf{x}	Independent variables
$\boldsymbol{\rho}$	Dependent variables
γ	Lagrange Multipliers
μ	Barrier parameter
$\mathbf{s}_1, \mathbf{s}_2$	Slack vectors
λ	Loading level

Bibliography

- [1] Kun Xiong and William D. Rosehart. Fast acting load control. *LESCOPE 02*, pages 23–28, July 2002.
- [2] Guang Li Steven M. Rovnyak, Kejun Mei. Fast load shedding for angle stability control. *IEEE Power Engineering Society General Meeting*, July 2003.
- [3] A. Wehbe and H. Salehfar. Direct Load Control for Reducing Losses in the Main and Laterals of Distribution System. *2002 IEEE*, pages 1593–1598, 2002.
- [4] D.Kottick Y.Halevi. Optimization of load shedding system. *IEEE Transactions on Energy Conversion*, (2):647–655, May 1992.
- [5] J. H. Doudna. Overview of California ISO Summer 2000 Demand Response Program. *Proc. of the IEEE PES General Meeting*, pages 16–1, January 2001.
- [6] J. H.Kehler. Procuring Load Curtailment for Grid Security in Alberta. *Proc. of the IEEE PES General Meeting*, pages 16–20, January 2001.
- [7] D. J. Lawrence. 2001 Performance of New York ISO Demand Response Programs. *Proc. of the IEEE PES General Meeting*, 18(2):46–50, January 2002.
- [8] Jason W. Black Marija Ilic and Jill L. Watz. Potential benefits of implementing load control. *IEEE Trans. Power Systems*, (2):177–182, May 2002.
- [9] W. Rosehart. Power system optimization with voltage stability constraints. Student poster session, 1998 IEEE/PES Summer Meeting, San Diego, CA, IEEE Power Engineering Review, Oct. 1998, pp. 14.

- [10] C. A. Cañizares. Applications of optimization to voltage collapse analysis. Panel Session, Optimization Techniques in Voltage Collapse Analysis, IEEE/PES Summer Meeting, San Diego, CA, Available at <http://www.power.uwaterloo.ca>, July 1998.
- [11] W. Rosehart, C. Cañizares, and V.H. Quintana. Optimal power flow incorporating voltage collapse constraints. Proc. of the 1999 IEEE/PES Summer Meeting, Edmonton, Alberta, July 1999, pp. 820-825.
- [12] Deqiang Gan and Eugene Litvinov. Energy and Reserve Market Designs with Explicit Consideration to Lost Opportunity Costs. *IEEE Trans. Power Systems*, 18(1):53–59, February 2003.
- [13] Alun H. Coonick Rabih A. Jabr and Brian J. Cory. A primal-dual interior point method for optimal power flow dispatching. *IEEE Trans, Power Systems*, 17(3):654–662, 2002.
- [14] S. Granville. Optimal reactive dispatch though interior point methods. *IEEE Trans. on Power Systems*, 11:136–146, 1996.
- [15] Power systems outages that occurred in the western interconnection on July 1996. *Tech. Rep., Western Systems Coordinating Council (WSCC)*, September 1996.
- [16] N.Mithulananthan. Voltage Stability Studay of the Sri Lankan power system grid. *Master's Thesis Asian Institute of Technology*, 1997.
- [17] David M. Gay Robert Fourer and Brian W. Kernighan. *AMPL: A Modeling Language for Mathematical Programming*. The Scientific Press, South San

Francisco, CA, 1993.

- [18] MathWorks. *Learning Matlab 6.5*. The MathWorks, Inc., 1984-2002.
- [19] R. J. Vanderbei. Loqo user's manual. Technical report, Princeton University, Princeton, New Jersey, 2000.
- [20] G. L. Torres and V. H. Quintana. An interior-point method for nonlinear optimal power flow using voltage rectangular coordinates. *IEEE Transactions on Power Systems*, pages 1211–1218, November 1998.
- [21] P. Kundur. *Power System Stability and Control*. McGraw Hill Publishing Company, New York, 1994.
- [22] Edward Wilson Kimbark. *Power System Stability*. McGraw Hill Publishing Company, New York, 1948.
- [23] C. A. Cañizares, editor. Voltage stability assessment: Concepts, practices and tools. Technical report, IEEE/PES Power System Stability Subcommittee, August 2002. available at <http://www.power.uwaterloo.ca>.
- [24] R. Seydel. *From Equilibrium to Chaos—Practical Bifurcation and Stability Analysis*. Elsevier Science, North-Holland, 1988.
- [25] A. A. P. Lerm, C. A. Cañizares, and A. S. e Silva. Multi-parameter bifurcation analysis of the south brazilian power system. accepted to *IEEE Trans. Power Systems*, May 2002.

- [26] I. Dobson and L. Lu. Voltage collapse precipitated by the immediate change in stability when generator reactive power limits are encountered. *IEEE Transactions on Circuits and Systems-I: Fundamental Theory and Applications*, 39(9):762–766, September 1992.
- [27] C. A. Cañizares and F. L. Alvarado. Point of collapse and continuation methods for large ac/dc systems. *IEEE Trans. Power Systems*, 8(1):1–8, February 1993.
- [28] V. Ajjarapu and C. Christy. The continuation power flow: A tool for steady state voltage stability analysis. *IEEE Trans. Power Systems*, 7(1):416–423, February 1992.
- [29] William D. Rosehart. *Optimization of power systems with voltage security constraints*. PhD thesis, University of Waterloo, Waterloo, Ontario, 2000.
- [30] W. Rosehart, C. Cañizares, and V.H. Quintana. Cost of voltage security in electricity markets. Proc. of the 2000 IEEE/PES Summer Meeting, Seattle, WA, July 2000, pp. 2115-2120.
- [31] Dimitri P. Bertsekas. *Nonlinear Programming*. Athena Scientific, Belmont, Massachusetts, 1995.
- [32] P.M. Pardalos. *Handbook of applied optimization / edited by Panos M. Pardalos and Mauricio G.C. Resende*. Oxford University Press, New York, 2002.
- [33] Philip E. Gill Anders Forsgren and Margaret H. Wright. *Interior Methods for Nonlinear Optimization*. 2002 Society for Industrial and Applied Mathematics, SIAM Review, December 2002.

- [34] Roy Marsten Gerg Astfalk, Irvin Lustig and David Shanno. The interior-point method for linear programming. *IEEE Software*, pages 61–88, July 1992.
- [35] Geraldo L. Torres and Victor H. Quintana. Optimal power flow via interior point methods: An educational tool in matlab. *IEEE*, 0-7803-3143-5:996–999, November 1996.
- [36] Antonio Gomez Exposito Jesus Riquelme, Alicia Troncoso Lora and Jose Luis Martinez Ramos. Finding improved local minima of power system optimization problems by interior point methods. *IEEE Trans. Power system*, 18:238–245, February 2003.
- [37] Geraldo L. Torres and Victor H. Quintana. An interior-point method for non-linear optimal power flow using voltage rectangular coordinates. *IEEE Trans. Power System*, 13:1211–1218, November 1998.
- [38] V.H. Quintana K. Ponnambalam and A. Vannelli. A fast algorithm for power system optimization problems using an interior point method. *IEEE*, 9(CH2948-8/91):393–399, 1991.
- [39] J.A. Momoh and J.A. Zhu. Improved interior point method for opf problem. *IEEE Trans, Power Systems*, 14(3):1114–1120, 1999.
- [40] University of Washington. Data archives. available at www.ee.washington.edu/research/pstca.
- [41] James E. Platts Robert B. Burke, Michael I. Henderson. Load response and system reliability. *IEEE Power Engineering Society General Meeting*, 2003.